

Quantum field theory of relic nonequilibrium systems

Nicolas G. Underwood* and Antony Valentini†

*Department of Physics and Astronomy, Clemson University,
Kinard Laboratory, Clemson, South Carolina 29634-0978, USA
(Received 21 November 2014; published 23 September 2015)*

In terms of the de Broglie-Bohm pilot-wave formulation of quantum theory, we develop field-theoretical models of quantum nonequilibrium systems which could exist today as relics from the very early Universe. We consider relic excited states generated by inflaton decay, as well as relic vacuum modes, for particle species that decoupled close to the Planck temperature. Simple estimates suggest that, at least in principle, quantum nonequilibrium could survive to the present day for some relic systems. The main focus of this paper is to describe the behavior of such systems in terms of field theory, with the aim of understanding how relic quantum nonequilibrium might manifest experimentally. We show by explicit calculation that simple perturbative couplings will transfer quantum nonequilibrium from one field to another (for example from the inflaton field to its decay products). We also show that fields in a state of quantum nonequilibrium will generate anomalous spectra for standard energy measurements. Possible connections to current astrophysical observations are briefly addressed.

DOI: [10.1103/PhysRevD.92.063531](https://doi.org/10.1103/PhysRevD.92.063531)

PACS numbers: 98.80.Cq

I. INTRODUCTION

In the de Broglie-Bohm pilot-wave formulation of quantum theory [1–4], the Born probability rule has a dynamical origin [5–11] and ordinary quantum physics is recovered as a special equilibrium case of a wider nonequilibrium physics [5–7,12–20]. On this view, we may understand the Born rule as arising from a relaxation process that took place in the remote past. Quantum nonequilibrium—that is, violations of the Born rule—may have existed in the very early universe before relaxation took place [5,6,12,13]. Such effects could leave observable traces today—in the cosmic microwave background (CMB) [15–18,21,22] or in relic systems that decoupled at very early times [7,15,16]. The former possibility has been developed in some detail and comparisons with data are beginning to be made [18,21–23]. The latter possibility is the focus of this paper.

According to our current understanding, the observed temperature anisotropy in the CMB was ultimately seeded by quantum fluctuations during an inflationary era [24–27]. Inflationary cosmology then provides us with an empirical window onto quantum probabilities in the very early Universe. On an expanding radiation-dominated background, relaxation in pilot-wave theory can be suppressed at long (super-Hubble) wavelengths while proceeding efficiently at short (sub-Hubble) wavelengths [15,16,18,21,22,28]. Thus, in a cosmology with a radiation-dominated preinflationary phase [29–33], one may obtain a large-scale or long-wavelength power deficit

in the CMB [15,16,18,21,22]. For an appropriate choice of cosmological parameters, the expected deficit is consistent with the deficit found in data from the *Planck* satellite [21,22,34]. Whether the observed deficit is in fact caused by quantum relaxation suppression during a preinflationary era or by some other more conventional effect remains to be seen.

A pilot-wave or de Broglie-Bohm treatment of the early Bunch-Davies vacuum shows that relaxation to quantum equilibrium does not take place at all during inflation itself [15,18]. Thus, if a residual nonequilibrium still existed at the end of a preinflationary era, the inflaton field would carry traces of that nonequilibrium forward to much later times. Similarly, should nonequilibrium be generated during the inflationary era by exotic gravitational effects at the Planck scale [18], the resulting departures from the Born rule will be preserved in the inflaton field and carried forward into the future where they might have an observable effect.

As we shall discuss in this paper, as well as imprinting a power deficit onto the CMB sky, a nonequilibrium inflaton field would also transfer nonequilibrium to the particles that are created by inflaton decay. Since such particles make up almost all of the matter present in our Universe, it seems conceivable that today there could exist relic particles that are still in a state of quantum nonequilibrium. We will also consider relic vacuum modes for other fields (apart from the inflaton) as potential carriers of nonequilibrium at late times.

These scenarios raise a number of immediate questions. First of all, even if nonequilibrium relics were created in the early Universe, could the nonequilibrium survive until late times and be detected today? As we shall see, simple estimates suggest that (at least in principle) relaxation to equilibrium could be avoided for some relic systems.

* nunderw@clemson.edu† Corresponding author.
antonyv@clemson.edu

A second question that must be addressed is the demonstration, in pilot-wave field theory, that perturbative interactions will in general transfer nonequilibrium from one field to another. This will be shown for a simplified model of quantum field theory involving just two energy levels for each field. Finally, one must ask what kind of new phenomena might be generated by relic nonequilibrium systems in an astrophysical or cosmological context. This opens up a potentially large domain of investigation. General arguments have already shown that the quantum-theoretical predictions for single-particle polarization probabilities (specifically Malus' law) would be broken for nonequilibrium systems [35]. In this paper we focus on measurements of energy as a simplified model of high-energy processes. It will be shown that conventional energy measurements performed on nonequilibrium systems would generate anomalous spectra. We may take this as a broad indication of the kinds of anomalies that would be seen in particle-physics processes taking place in the presence of quantum nonequilibrium.

In this paper we are not concerned with the question of practical detection of relic nonequilibrium. Rather, our intention is to make a case that detection might be possible at least in principle, and to begin the development of field-theoretical models of the behavior of relic nonequilibrium matter.

Generally speaking, even a lowest-order calculation of perturbative processes in quantum field theory will involve all of the field modes that are present in the system. While such calculations are in principle possible in de Broglie-Bohm theory, in practice it would involve integrating trajectories for an unlimited number of field modes. In this paper, we make a beginning by confining ourselves to simplified or truncated models of quantum field theory involving only a small number of field modes. Our models are inspired by approximations commonly used in quantum optics, where one is often interested in the dynamics of a single (quantized) electromagnetic field mode inside a cavity. Our main aim is to justify the assertions that underpin our scenarios. In particular, we wish to show by explicit calculation of examples that perturbative couplings will in general transfer nonequilibrium from one field to another, and that nonequilibrium will affect the spectra for basic particle-physics processes involving measurements of energy. We emphasize that the calculations presented in this paper are only intended to be broadly illustrative. The development of more realistic models is left for future work.

In Sec. II A we summarize the background to our scenario, and in particular the justification for why the inflaton field singles itself out as a natural carrier of primordial quantum nonequilibrium. In Sec. II B we argue that inflaton decay can generate particles in a state of quantum nonequilibrium (induced by nonequilibrium inflaton perturbations and also by the other nonequilibrium

degrees of freedom that can exist in the vacuum), and that such nonequilibrium could in principle survive to the present day for those decay particles that were created at times later than the relevant decoupling time. The gravitino provides a suggestive, or at least illustrative, candidate. In Sec. II C we consider a somewhat simpler scenario involving relic nonequilibrium field modes for the vacuum only. For simplicity we restrict ourselves to conformally coupled fields, as these will not be excited by the spatial expansion. It is argued that super-Hubble vacuum modes that enter the Hubble radius after the decoupling time for the corresponding particle species will remain free of interactions and could potentially carry traces of primordial nonequilibrium to the present day (for sufficiently long comoving wavelengths). An illustrative example is provided by the massless gravitino. In Sec. II D we indicate how particle-physics processes would be affected by a nonequilibrium vacuum.

These preliminary considerations provide motivation for the subsequent detailed calculations. In Sec. III we give an example of the perturbative transfer of nonequilibrium from one field to another, a process that could play a role in inflaton decay as well as in the decay of relic nonequilibrium particles generally. In Sec. IV we provide a field-theoretical model of energy measurements, and we show by detailed calculation of various examples that nonequilibrium will entail corrections to the energy spectra generated by high-energy physics processes. Finally, in Sec. V we present our conclusions. We briefly address the possible relevance of our scenarios to current searches for dark matter. We also comment on some practical obstacles to detecting relic nonequilibrium (even if it exists) and we emphasize the gaps in our scenarios that need to be filled in future work.

II. RELIC NONEQUILIBRIUM SYSTEMS

In this section we first summarize the background to our scenario and in particular the role that quantum nonequilibrium might play in the very early universe. We then provide some simple arguments suggesting that primordial violations of the Born rule might survive until much later epochs and perhaps even to the present day [28]. These arguments motivate the detailed analysis of nonequilibrium systems provided later in the paper.

A. Nonequilibrium primordial perturbations

In de Broglie-Bohm pilot-wave theory [1–4], a system has a configuration $q(t)$ whose velocity $\dot{q} \equiv dq/dt$ is determined by the wave function $\psi(q, t)$. As usual, ψ obeys the Schrödinger equation $i\partial\psi/\partial t = \hat{H}\psi$ (with $\hbar = 1$). For standard Hamiltonians \dot{q} is proportional to the phase gradient $\text{Im}(\partial_q\psi/\psi)$. Quite generally,

$$\frac{dq}{dt} = \frac{j}{|\psi|^2}, \quad (1)$$

where $j = j[\psi] = j(q, t)$ is the Schrödinger current [36]. The configuration-space “pilot wave” ψ guides the motion of an individual system and has no intrinsic connection with probabilities. For an ensemble with the same wave function we may consider an arbitrary distribution $\rho(q, t)$ of configurations $q(t)$. By construction, $\rho(q, t)$ will satisfy the continuity equation

$$\frac{\partial \rho}{\partial t} + \partial_q \cdot (\rho \dot{q}) = 0. \quad (2)$$

Because $|\psi|^2$ obeys the same equation, an initial “quantum equilibrium” distribution $\rho(q, t_i) = |\psi(q, t_i)|^2$ trivially evolves into a final quantum equilibrium distribution $\rho(q, t) = |\psi(q, t)|^2$. In equilibrium we obtain the Born rule and the usual empirical predictions of quantum theory [2,3]. Whereas, for a nonequilibrium ensemble ($\rho(q, t) \neq |\psi(q, t)|^2$), the statistical predictions will generally differ from those of quantum theory [5–7,12–20].

If they existed, nonequilibrium distributions would generate new phenomena that lie outside the domain of conventional quantum theory. This new physics would allow nonlocal signalling [12]—which is causally consistent with an underlying preferred foliation of spacetime [37]—and it would also allow “subquantum” measurements that violate the uncertainty principle and other standard quantum constraints [14,20].

The equilibrium state $\rho = |\psi|^2$ arises from a dynamical process of relaxation (roughly analogous to thermal relaxation). This may be quantified by an H -function $H = \int dq \rho \ln(\rho/|\psi|^2)$ [5–7]. Extensive numerical simulations have shown that when ψ is a superposition of energy eigenstates there is rapid relaxation $\rho \rightarrow |\psi|^2$ (on a coarse-grained level) [6–11,38], with an approximately exponential decay of the coarse-grained H -function with time [8,10,38]. In this way, the Born rule arises from a relaxation process that presumably took place in the very early Universe [5,6,12,13]. While ordinary laboratory systems—which have a long and violent astrophysical history—are expected to obey the equilibrium Born rule to high accuracy, quantum nonequilibrium in the early Universe can leave an imprint in the CMB [15,18,21,22] and perhaps even survive in relic particles that decoupled at sufficiently early times [7,15,16]. The latter possibility provides the subject matter of this paper.

Much of the physics may be illustrated by the dynamics of a massless, minimally coupled and real scalar field ϕ evolving freely on an expanding background with line element $d\tau^2 = dt^2 - a^2 d\mathbf{x}^2$ [where $a = a(t)$ is the scale factor and we take $c = 1$]. Beginning with the classical Lagrangian density

$$\mathcal{L} = \frac{1}{2} \sqrt{-g} g^{\mu\nu} \partial_\mu \phi \partial_\nu \phi, \quad (3)$$

where $g_{\mu\nu}$ is the background metric, and working with Fourier components $\phi_{\mathbf{k}} = \frac{\sqrt{V}}{(2\pi)^{3/2}} (q_{\mathbf{k}1} + i q_{\mathbf{k}2})$ —where V is a normalization volume and $q_{\mathbf{k}r}$ ($r = 1, 2$) are real variables—the field Hamiltonian becomes a sum $H = \sum_{\mathbf{k}r} H_{\mathbf{k}r}$ where

$$H_{\mathbf{k}r} = \frac{1}{2a^3} \pi_{\mathbf{k}r}^2 + \frac{1}{2} a k^2 q_{\mathbf{k}r}^2 \quad (4)$$

is formally the Hamiltonian of a harmonic oscillator with mass $m = a^3$ and angular frequency $\omega = k/a$. Straightforward quantization then yields the Schrödinger equation

$$i \frac{\partial \Psi}{\partial t} = \sum_{\mathbf{k}r} \left(-\frac{1}{2a^3} \frac{\partial^2}{\partial q_{\mathbf{k}r}^2} + \frac{1}{2} a k^2 q_{\mathbf{k}r}^2 \right) \Psi \quad (5)$$

for the wave functional $\Psi = \Psi[q_{\mathbf{k}r}, t]$, from which one may identify the de Broglie guidance equation

$$\frac{dq_{\mathbf{k}r}}{dt} = \frac{1}{a^3} \text{Im} \frac{1}{\Psi} \frac{\partial \Psi}{\partial q_{\mathbf{k}r}} \quad (6)$$

for the evolving degrees of freedom $q_{\mathbf{k}r}$ [15,16,18]. (We have assumed a preferred foliation of spacetime with time function t . A similar construction may be given in any globally hyperbolic spacetime [28,37,39].)

An unentangled mode \mathbf{k} has an independent dynamics with wave function $\psi_{\mathbf{k}}(q_{\mathbf{k}1}, q_{\mathbf{k}2}, t)$. The equations are the same as those for a nonrelativistic two-dimensional harmonic oscillator with time-dependent mass $m = a^3$ and time-dependent angular frequency $\omega = k/a$. Thus we may discuss relaxation for a single field mode in terms of relaxation for such an oscillator [15,16]. It has been shown that the time evolution is mathematically equivalent to that of a standard oscillator (with constant mass and constant angular frequency) but with real time t replaced by a “retarded time” $t_{\text{ret}}(t)$ that depends on the wave number k [21]. Thus, in effect, cosmological relaxation for a single field mode may be discussed in terms of relaxation for a standard oscillator.

Cosmological relaxation has been studied in detail for the case of a radiation-dominated expansion, with $a \propto t^{1/2}$ [21,22]. In the short-wavelength or sub-Hubble limit, it is found that $t_{\text{ret}}(t) \rightarrow t$ and so we obtain the time evolution of a field mode on Minkowski spacetime, with rapid relaxation taking place for a superposition of excited states. On the other hand, for long (super-Hubble) wavelengths it is found that $t_{\text{ret}}(t) \ll t$ and so relaxation is retarded.¹ Thus, in a cosmology with a radiation-dominated preinflationary era, at the onset of inflation we may reasonably expect to

¹Such retardation may also be described in terms of the mean displacement of the trajectories [16,28].

find relic nonequilibrium at sufficiently large wavelengths [18,21,22].

No further relaxation takes place during inflation itself. This has been shown by calculating the de Broglie-Bohm trajectories of the inflaton field in the Bunch-Davies vacuum [15,18]. In terms of conformal time $\eta = -1/Ha$, the wave functional is simply a product $\Psi[q_{\mathbf{k}r}, \eta] = \prod_{\mathbf{k}r} \psi_{\mathbf{k}r}(q_{\mathbf{k}r}, \eta)$ of contracting Gaussian packets and the trajectories take the simple form $q_{\mathbf{k}r}(\eta) = q_{\mathbf{k}r}(0) \sqrt{1 + k^2 \eta^2}$. The time evolution of an arbitrary nonequilibrium distribution $\rho_{\mathbf{k}r}(q_{\mathbf{k}r}, \eta)$ then amounts trivially to the same overall contraction that occurs for the equilibrium distribution. It follows that the width of the evolving nonequilibrium distribution remains in a constant ratio with the width of the evolving equilibrium distribution. Thus the ratio

$$\xi(k) \equiv \frac{\langle |\phi_{\mathbf{k}}|^2 \rangle}{\langle |\phi_{\mathbf{k}}|^2 \rangle_{\text{QT}}} \quad (7)$$

of the nonequilibrium variance $\langle |\phi_{\mathbf{k}}|^2 \rangle$ to the quantum-theoretical variance $\langle |\phi_{\mathbf{k}}|^2 \rangle_{\text{QT}}$ is preserved in time. Any relic nonequilibrium ($\xi \neq 1$) that exists at the beginning of inflation is preserved during the inflationary era and is simply transferred to larger length scales as physical wavelengths $\lambda_{\text{phys}} = a\lambda = a(2\pi/k)$ grow with time.

It follows that incomplete relaxation at long wavelengths during a preinflationary era can change the spectrum of perturbations during inflation and thus affect the primordial power spectrum for the curvature perturbations that seed the temperature anisotropy in the CMB. An inflaton perturbation $\phi_{\mathbf{k}}$ generates a curvature perturbation $\mathcal{R}_{\mathbf{k}} \propto \phi_{\mathbf{k}}$ (where $\phi_{\mathbf{k}}$ is evaluated at a time a few e -folds after the mode exits the Hubble radius) [24]. This in turn generates the observed angular power spectrum

$$C_l = \frac{1}{2\pi^2} \int_0^\infty \frac{dk}{k} T^2(k, l) \mathcal{P}_{\mathcal{R}}(k) \quad (8)$$

for the CMB, where $T(k, l)$ is the transfer function and

$$\mathcal{P}_{\mathcal{R}}(k) \equiv \frac{4\pi k^3}{V} \langle |\mathcal{R}_{\mathbf{k}}|^2 \rangle \quad (9)$$

is the primordial power spectrum. From (7) we have

$$\mathcal{P}_{\mathcal{R}}(k) = \mathcal{P}_{\mathcal{R}}^{\text{QT}}(k) \xi(k), \quad (10)$$

where $\mathcal{P}_{\mathcal{R}}^{\text{QT}}(k)$ is the quantum-theoretical or equilibrium power spectrum. Thus measurements of C_l may be used to set experimental limits on $\xi(k)$ [18].

The function $\xi(k)$ quantifies the degree of nonequilibrium as a function of k . In a model with a preinflationary era, extensive numerical simulations show that $\xi(k)$ is expected to take the form of an inverse-tangent—with

$\xi < 1$ for small k and $\xi \simeq 1$ at large k [22]. The extent to which this prediction is supported by the data is currently under study [23].

Incomplete relaxation in the past is one means by which nonequilibrium could exist in the inflationary era. Another possibility is that nonequilibrium is *generated* during the inflationary phase by exotic gravitational effects at the Planck scale (Ref. [18], Sec. IV B). Trans-Planckian modes—that is, modes that originally had sub-Planckian physical wavelengths—may well contribute to the observable part of the inflationary spectrum [40,41], in which case inflation provides an empirical window onto physics at the Planck scale [42]. It has been suggested that quantum equilibrium might be gravitationally unstable [15,39]. In quantum field theory the existence of an equilibrium state arguably requires a background spacetime that is globally hyperbolic, in which case nonequilibrium could be generated by the formation and evaporation of a black hole (a proposal that is also motivated by the controversial question of information loss) [15,39]. A heuristic picture of the formation and evaporation of microscopic black holes then suggests that quantum nonequilibrium will be generated at the Planck length l_p . Such a process could be modeled in terms of nonequilibrium field modes. Thus, a mode that begins with a physical wavelength $\lambda_{\text{phys}} < l_p$ in the early inflationary era may be assumed to be out of equilibrium upon exiting the Planckian regime (that is, when $\lambda_{\text{phys}} > l_p$) [18]. If such processes exist, the inflaton field will carry quantum nonequilibrium at *short* wavelengths (below some comoving cutoff).

For our present purpose, the main conclusion to draw is that the inflaton field may act as a carrier of primordial nonequilibrium—whether it is relic nonequilibrium from incomplete relaxation during a preinflationary era, or nonequilibrium that was generated by Planck-scale effects during inflation itself. This brings us to the question: in addition to leaving a macroscopic imprint on the CMB, could primordial nonequilibrium survive all the way up to the present and be found in microscopic relic systems today?.

B. Inflaton decay

Postinflation, the density of any relic particles (nonequilibrium or otherwise) from a preinflationary era will be so diluted as to be completely undetectable today. However, one may consider relic particles that were created at the end of inflation by the decay of the inflaton field itself—where in standard inflationary scenarios inflaton decay is in fact the source of almost all the matter present in our Universe.

To discuss this, note that in pilot-wave theory it is standard to describe bosonic fields in terms of evolving field configurations (as in our treatment of the free scalar field in Sec. II A) whereas there are different approaches for fermionic fields. Arguably the most straightforward pilot-wave theory of fermions utilizes a Dirac sea picture of

particle trajectories determined by a pilot wave that obeys the many-body Dirac equation [43–45]. Alternatively, a formal field theory based on anticommuting Grassmann fields may be written down [6,13] but its interpretation presents problems that remain to be addressed [46]. For our purposes we will assume the Dirac sea model for fermions.

During the inflationary era the inflaton field φ is approximately homogeneous and may be written as

$$\varphi(\mathbf{x}, t) = \phi_0(t) + \phi(\mathbf{x}, t), \quad (11)$$

where $\phi_0(t)$ is a homogeneous part and $\phi(\mathbf{x}, t)$ [or $\phi_{\mathbf{k}}(t)$] is a small perturbation. As we have noted, during the inflationary expansion perturbations $\phi_{\mathbf{k}}$ do not relax to quantum equilibrium and in fact the exponential expansion of space transfers any nonequilibrium that may exist from microscopic to macroscopic length scales. The inflaton field is then a natural candidate for a carrier of primordial quantum nonequilibrium (whatever its ultimate origin).

The process of “preheating” is driven by the homogeneous and essentially classical part $\phi_0(t)$ (that is, by the $k = 0$ mode of the inflaton field) [47]. The inflaton is treated as a classical external field, acting on other (quantum) fields which become excited by parametric resonance. Because of the classicality of the relevant part of the inflaton field, this process is unlikely to result in a transference of nonequilibrium from the inflaton to the created particles. During “reheating”, however, perturbative decay of the inflaton can occur, and we expect that nonequilibrium in the inflaton field will be at least to some extent transferred to its decay products.

Note that we follow the standard procedure of treating the large homogeneous part $\phi_0(t)$ as a classical field and the small perturbation $\phi(\mathbf{x}, t)$ as a quantized field. This deserves some comment. In the context of preheating, it has been argued that $\phi_0(t)$ arises from a coherent state with a space-independent quantum expectation value [48]. It is also common to argue that the large amplitude and large occupation number of the “zero mode” at the end of inflation justifies it being treated as a classical field (see for example Refs. [47] and [49]). Here we assume the standard formalism, albeit rewritten in de Broglie-Bohm form. By construction, then, there is no probability distribution for $\phi_0(t)$ (which has a classical “known” value at all times). Whereas $\phi(\mathbf{x}, t)$ has a probability distribution, which in the standard theory is given by the Born rule and which in de Broglie-Bohm theory can be more general. The probability distribution for $\phi(\mathbf{x}, t)$ is used to calculate the power spectrum emerging from the inflationary vacuum. By allowing this distribution to be out of equilibrium, new physical effects can occur in the CMB [18]. In contrast, because $\phi_0(t)$ is treated as a classical background field with no probability distribution there is no question of ascribing equilibrium or nonequilibrium to this part of the field (at

least not at the level of the effective description which we adopt here).²

The perturbative decay of the inflaton occurs through local interactions. For example, reheating can occur if the inflaton field φ is coupled to a bosonic field Φ and a fermionic field ψ via an interaction Hamiltonian density of the form

$$\mathcal{H}_{\text{int}} = a\varphi\Phi^2 + b\varphi\bar{\psi}\psi, \quad (12)$$

where a, b are constants (Ref. [27], p. 507). In actual calculations, it is usual to consider only the dominant homogeneous part ϕ_0 of the field $\varphi = \phi_0 + \phi$, and to ignore contributions from the small perturbation ϕ . Because the dominant homogeneous part ϕ_0 is treated essentially classically, inflaton decay bears some resemblance to the process of pair creation by a strong classical electric field.

The decay particles will have physical wavelengths no greater than the instantaneous Hubble radius, $\lambda_{\text{phys}} \lesssim H^{-1}$, since local processes cannot significantly excite super-Hubble modes (for which the particle concept is in any case ill-defined). This standard argument—that super-Hubble modes are shielded from the effects of local interactions—is still valid in the de Broglie-Bohm formulation since we are speaking of the time evolution of the wave functional Ψ (and of its mode decomposition) which still satisfies the usual Schrödinger equation. We have a nonlocal dynamical Eq. (1) for the evolving configuration $q(t)$, but the Schrödinger equation for Ψ takes the usual form and therefore has the usual properties. Local Hamiltonian terms in the Schrödinger equation will be unable to excite super-Hubble modes just as in standard quantum field theory.

How could quantum nonequilibrium exist in the decay products? There seem to be two possible mechanisms.

First, note that the inflaton perturbation ϕ will also appear in the interaction Hamiltonian (12). The dominant processes of particle creation by the homogeneous part ϕ_0 will necessarily be subject to corrections from the perturbation ϕ . If the perturbation is out of equilibrium, the induced corrections will carry signatures of nonequilibrium—as will be illustrated by a simple model of field couplings in Sec. III.

Second, as in any de Broglie-Bohm account of a quantum process, the final probability distribution for the created particles will originate from the initial probability distribution for the *complete* hidden-variable state.³

²Note that, in the standard formalism being assumed here, even at very long wavelengths there remains a formal distinction between the large classical homogeneous field $\phi_0(t)$ and modes of the small quantized field $\phi(\mathbf{x}, t)$.

³In pilot-wave theory the outcome of a single quantum measurement is determined by the complete initial configuration (together with the initial wave function and total Hamiltonian). Over an ensemble, the distribution of outcomes is then determined by the distribution of initial configurations.

In this case the initial hidden-variable state will include vacuum bosonic field configurations together with vacuum fermionic particle configurations for the created species (assuming a Dirac-sea account of fermions). Thus, if the relevant vacuum variables for the created species are out of equilibrium at the beginning of inflaton decay, the created particles will in general violate the Born rule. As we have discussed, inflaton perturbations do not relax to equilibrium during the inflationary phase. One may expect that the other degrees of freedom in the vacuum will show a comparable behavior—in which case they could indeed be out of equilibrium at the onset of inflaton decay, resulting in nonequilibrium for the decay products.

At least in principle, then, the particles created by inflaton decay could show deviations from quantum equilibrium. However, subsequent relaxation can be avoided only if the particles are created at a time after their corresponding decoupling time t_{dec} (when the mean free time t_{col} between collisions is larger than the expansion time scale $t_{\text{exp}} \equiv a/\dot{a}$) or equivalently at a temperature below their decoupling temperature T_{dec} . Otherwise the interactions with other particles are likely to cause rapid relaxation.

A natural candidate to consider is the gravitino \tilde{G} , which arises in supersymmetric theories of high-energy physics. In some models, gravitinos are copiously produced by inflaton decay [50–52] and could make up a significant component of dark matter [53]. (For recent reviews of gravitinos as dark matter candidates see for example Refs. [54,55].) Gravitinos are very weakly interacting and therefore in practice could not be detected directly, but in many models they are unstable and decay into particles that are more readily detectable. Again, as we shall see, in general we expect any decay process to transfer quantum nonequilibrium from the initial decaying field to the decay products. Thus, at least in principle, one could search for deviations from the Born rule in (say) photons that are generated by gravitino decay. However, the decay would have to take place after the time $(t_{\text{dec}})_{\gamma}$ of photon decoupling—so that the decay photons may in turn avoid relaxation.

It may then seem unlikely that primordial nonequilibrium could ever survive until the present, since several stages may be required. But simple estimates suggest that at least in principle the required constraints could be satisfied for some models.

The unstable gravitino \tilde{G} has been estimated to decouple at a temperature $(T_{\text{dec}})_{\tilde{G}}$ given by [56]

$$\begin{aligned} k_{\text{B}}(T_{\text{dec}})_{\tilde{G}} &\equiv x_{\tilde{G}}(k_{\text{B}}T_{\text{P}}) \\ &\approx (1 \text{ TeV}) \left(\frac{g_*}{230}\right)^{1/2} \left(\frac{m_{\tilde{G}}}{10 \text{ keV}}\right)^2 \left(\frac{1 \text{ TeV}}{m_{\text{gl}}}\right)^2, \end{aligned} \quad (13)$$

$$(14)$$

where T_{P} is the Planck temperature, g_* is the number of spin degrees of freedom (for the effectively massless particles) at

the temperature $(T_{\text{dec}})_{\tilde{G}}$, m_{gl} is the gluino mass, and $m_{\tilde{G}}$ is the gravitino mass. For the purpose of illustration, if we take $(g_*/230)^{1/2} \sim 1$ and $(1 \text{ TeV}/m_{\text{gl}})^2 \sim 1$, then

$$x_{\tilde{G}} \approx \left(\frac{m_{\tilde{G}}}{10^3 \text{ GeV}}\right)^2. \quad (15)$$

If for example we take $m_{\tilde{G}} \approx 100 \text{ GeV}$, then $x_{\tilde{G}} \approx 10^{-2}$. Gravitinos produced by inflaton decay at temperatures below $(T_{\text{dec}})_{\tilde{G}} \equiv x_{\tilde{G}}T_{\text{P}}$ could potentially avoid quantum relaxation. Any nonequilibrium which they carry could then be transferred to their decay products. If the gravitino is not the lightest supersymmetric particle, then it will indeed be unstable. For large $m_{\tilde{G}}$ the total decay rate is estimated to be [57]

$$\Gamma_{\tilde{G}} = (193/48)(m_{\tilde{G}}^3/M_{\text{P}}^2), \quad (16)$$

where $M_{\text{P}} \approx 1.2 \times 10^{19} \text{ GeV}$ is the Planck mass. The time $(t_{\text{decay}})_{\tilde{G}}$ at which the gravitino decays is of order the lifetime $1/\Gamma_{\tilde{G}}$. Using the standard temperature-time relation

$$t \sim (1 \text{ s}) \left(\frac{1 \text{ MeV}}{k_{\text{B}}T}\right)^2, \quad (17)$$

the corresponding temperature is then

$$k_{\text{B}}(T_{\text{decay}})_{\tilde{G}} \sim (m_{\tilde{G}}/1 \text{ GeV})^{3/2} \text{ eV}. \quad (18)$$

For example, again for the case $m_{\tilde{G}} \approx 100 \text{ GeV}$, the relic gravitinos will decay when $k_{\text{B}}(T_{\text{decay}})_{\tilde{G}} \sim 1 \text{ keV}$. This is prior to photon decoupling, so that any (potentially non-equilibrium) photons produced by the decaying gravitinos would interact strongly with matter and quickly relax to quantum equilibrium. To obtain gravitino decay after photon decoupling, we would need $k_{\text{B}}(T_{\text{decay}})_{\tilde{G}} \lesssim k_{\text{B}}(T_{\text{dec}})_{\gamma} \sim 0.3 \text{ eV}$, or $m_{\tilde{G}} \lesssim 0.5 \text{ GeV}$. For such small gravitino masses, decoupling occurs at (roughly)

$$(T_{\text{dec}})_{\tilde{G}} = x_{\tilde{G}}T_{\text{P}} \approx (m_{\tilde{G}}/10^3 \text{ GeV})^2 T_{\text{P}} \lesssim 10^{-7} T_{\text{P}}. \quad (19)$$

In such a scenario, to have a hope of finding relic nonequilibrium in photons from gravitino decay, we would need to restrict ourselves to those gravitinos that were produced by inflaton decay at temperatures $\lesssim 10^{-7} T_{\text{P}}$.

Our considerations here are intended to be illustrative only. It may prove more favorable to consider other gravitino decay products—or to apply similar reasoning to other relics from the Planck era besides the gravitino.⁴

⁴Colin [58] has developed the pilot-wave theory of (first-quantized) Majorana fermions and suggests that quantum nonequilibrium might survive at sub-Compton length scales for these systems.

And of course one could also consider photons that are generated by the annihilation of relic particles as well as by their decay.

While definite conclusions must await the development of detailed and specific models, in principle the required constraints do not seem insuperable. There is, however, a further question we have yet to address: whether or not relaxation will still occur even for decay particles that are decoupled. Decoupling is necessary but not sufficient to avoid relaxation. We may discuss this for decay particles whose physical wavelengths are sufficiently sub-Hubble ($\lambda_{\text{phys}} \ll H^{-1}$) that the Minkowski limit applies, since extensive numerical studies of relaxation have already been carried out in this limit. If the decay particles are free but in quantum states that are superpositions of even modest numbers of energy eigenstates, then rapid relaxation will occur (on time scales comparable to those over which the wave function itself evolves) [6–11,38]. On the other hand, if the number of energy states in the superposition is small then it is likely that relaxation will not take place completely. It was shown in Ref. [38] that, if the relative phases in the initial superposition are chosen randomly, then for small numbers of energy states it is likely that the trajectories will not fully explore the configuration space, resulting in a small but significant nonzero “residue” in the coarse-grained H -function—corresponding to a small deviation from quantum equilibrium—even in the long-time limit. It appears that such behavior can occur for larger numbers of energy states as well, but will be increasingly rare the more energy states are present in the superposition (see Ref. [38] for a detailed discussion). Decay particles will be generated with a range of effective quantum states. For that fraction of particles whose wave functions have a small number of superposed energy states, there is likely to be a small residual nonequilibrium even in the long-time limit. Therefore, again, at least in principle there seems to be no insuperable obstacle to primordial nonequilibrium surviving to some (perhaps small) degree until the present day.

C. Relic conformal vacua

While inflaton decay will certainly create nonequilibrium particles from an initially nonequilibrium vacuum, we have seen that there are practical obstacles to such nonequilibrium surviving until the present day. The obstacles do not seem insurmountable in principle, but whether a scenario of the kind we have sketched will be realized in practice is at present unknown. There is, however, an alternative and rather simpler scenario which appears to be free of such obstacles. This involves considering relic nonequilibrium field modes for the vacuum only. This has the advantage that vacuum wave functions are so simple that no further relaxation can be generated—any relic nonequilibrium from earlier times will be frozen and preserved.

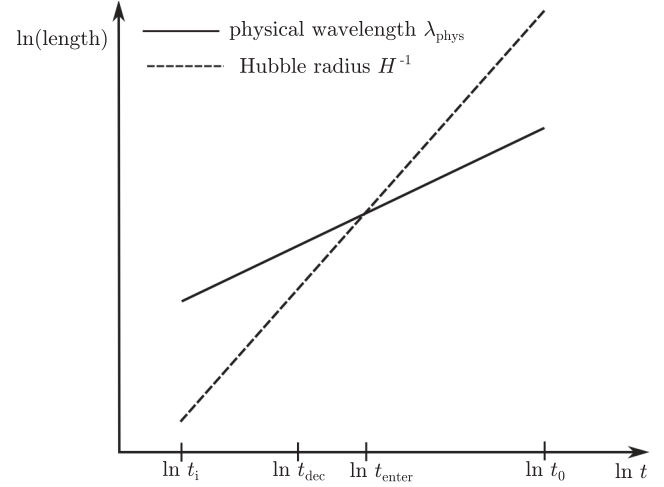


FIG. 1. Length scales for a radiation-dominated expansion. The solid line shows the time evolution of the physical wavelength $\lambda_{\text{phys}} = a\lambda \propto t^{1/2}$. The dashed line shows the time evolution of the Hubble radius $H^{-1} = 2t$. The mode enters the Hubble radius after the decoupling time t_{dec} .

But how could primordial field modes remain unexcited in the postinflationary era? For a given field there are three mechanisms that can cause excitation: (i) inflaton decay, (ii) interactions with other fields, and (iii) spatial expansion. It is, however, possible to avoid each of these. Firstly, while a field mode is in the super-Hubble regime it will in effect be shielded from the effects of local physics and will not be subject to excitation from perturbative interactions (with the inflaton or with other fields).⁵ Secondly, if during the postinflationary radiation-dominated phase the field mode enters the Hubble radius at a time t_{enter} that is later than the decoupling time t_{dec} for the corresponding particle species, the mode will remain free of interactions and continue to be unexcited (see Fig. 1). Finally, the effects of spatial expansion may be avoided altogether by restricting our attention to fields that are conformally coupled to the spacetime metric. For example, for a massless scalar field ϕ with Lagrangian density

$$\mathcal{L} = \frac{1}{2} \sqrt{-g} \left(g_{\mu\nu} \partial^\mu \phi \partial^\nu \phi - \frac{1}{6} R \phi^2 \right) \quad (20)$$

(where R is the curvature scalar), the dynamics is invariant under a conformal transformation $g_{\mu\nu}(x) \rightarrow \tilde{g}_{\mu\nu}(x) = \Omega^2(x) g_{\mu\nu}(x)$, $\phi(x) \rightarrow \tilde{\phi}(x) = \Omega^{-1}(x) \phi(x)$, where $\Omega(x)$ is an arbitrary spacetime function [59,60]. Because a Friedmann–Lemaître spacetime is conformally related to a section of Minkowski spacetime, the spatial expansion will not create particles for a (free) conformally coupled

⁵Again, this standard argument is still valid in the de Broglie–Bohm formulation since we are referring to the time evolution of the wave functional only.

field. The natural or conformal vacuum state is stable, just as in Minkowski spacetime [59,60]. Conformal invariance is however possible only for massless fields, whether bosonic or fermionic. As examples of conformally coupled particle species, we may consider photons and (if they exist) massless neutrinos and massless gravitinos.

Because ground-state wave functions and the associated de Broglie velocity fields are so simple (indeed trivial), relic vacuum modes will not relax to equilibrium and could therefore survive as carriers of nonequilibrium until the present day. As we shall see, nonequilibrium vacuum modes would in principle generate corrections to particle-physics processes.

At what length scale might relic nonequilibrium exist in the vacuum today? This may be estimated by requiring that the modes enter the Hubble radius at times $t_{\text{enter}} > t_{\text{dec}}$ (so as to avoid excitation and hence likely relaxation). Thus we require that at the time t_{dec} the vacuum modes have an instantaneous physical wavelength $\lambda_{\text{phys}}^{\text{vac}}(t_{\text{dec}})$ that is super-Hubble,

$$\lambda_{\text{phys}}^{\text{vac}}(t_{\text{dec}}) \gtrsim H_{\text{dec}}^{-1}, \quad (21)$$

where H_{dec}^{-1} is the Hubble radius at time t_{dec} (as shown in Fig. 1). Now $\lambda_{\text{phys}}^{\text{vac}}(t_{\text{dec}}) = a_{\text{dec}} \lambda^{\text{vac}}$ (where $a_{\text{dec}} = T_0/T_{\text{dec}}$ and $T_0 \approx 2.7$ K) and $H_{\text{dec}}^{-1} = 2t_{\text{dec}}$ with t_{dec} expressed in terms of T_{dec} by the approximate formula (17). The lower bound (21) then becomes (inserting c)

$$\lambda^{\text{vac}} \gtrsim 2c(1 \text{ s}) \left(\frac{1 \text{ MeV}}{k_{\text{B}} T_{\text{dec}}} \right) \left(\frac{1 \text{ MeV}}{k_{\text{B}} T_0} \right) \quad (22)$$

or

$$\lambda^{\text{vac}} \gtrsim (3 \times 10^{20} \text{ cm}) \left(\frac{1 \text{ MeV}}{k_{\text{B}} T_{\text{dec}}} \right). \quad (23)$$

This is a lower bound on the comoving wavelength λ^{vac} at which nonequilibrium could be found for conformally coupled vacuum modes.

The lower bound (23) becomes prohibitively large unless we focus on fields that decouple around the Planck temperature or soon after. For photons $k_{\text{B}}(T_{\text{dec}})_{\gamma} \sim 0.3$ eV, and so for the electromagnetic vacuum (23) implies $\lambda_{\gamma}^{\text{vac}} \gtrsim 10^{27}$ cm. For massless, conformally coupled neutrinos (if such exist), $k_{\text{B}}(T_{\text{dec}})_{\nu} \sim 1$ MeV and $\lambda_{\nu}^{\text{vac}} \gtrsim 10^{20}$ cm ≈ 30 pc (or $\sim 10^2$ light years). Relic nonequilibrium for these vacua could plausibly exist today only at such huge wavelengths and any induced effects would be far beyond any range of detection in the foreseeable future.

We must therefore consider fields that decoupled close to the Planck temperature. Gravitons are expected to be minimally coupled and so would not have a stable vacuum state under the spatial expansion. However, a massless

gravitino field should be conformally coupled, in which case it would be a candidate for our scenario. For massless gravitinos we have a lower bound

$$\lambda_{\tilde{G}}^{\text{vac}} \gtrsim (10^{-2} \text{ cm})(1/x_{\tilde{G}}) \quad (24)$$

[again writing $k_{\text{B}}(T_{\text{dec}})_{\tilde{G}} \equiv x_{\tilde{G}}(k_{\text{B}} T_{\text{P}}) \approx x_{\tilde{G}}(10^{19} \text{ GeV})$ and with $x_{\tilde{G}} \lesssim 1$]. If, for example, we take $x_{\tilde{G}} \approx 10^{-2}$ then $\lambda_{\tilde{G}}^{\text{vac}} \gtrsim 1$ cm. According to this crude and illustrative estimate, relic nonequilibrium for a massless gravitino vacuum today appears to be possible for modes of wavelength $\gtrsim 1$ cm.

D. Particle physics in a nonequilibrium vacuum

If nonequilibrium vacuum modes do exist today, how could they manifest experimentally? In principle they would induce nonequilibrium corrections to particle creation from the vacuum (as already noted for inflaton decay) or to other perturbative processes such as particle decay.

Consider for example a free scalar field $\Phi(\mathbf{x}, t)$ that is massive and charged. Let us again write the Fourier components as $\Phi_{\mathbf{k}}(t) = (\sqrt{V}/(2\pi)^{3/2})(Q_{\mathbf{k}1}(t) + iQ_{\mathbf{k}2}(t))$ with real $Q_{\mathbf{k}r}$ ($r = 1, 2$). In Minkowski spacetime—which is suitable for a description of local laboratory physics—the vacuum wave functional takes the form

$$\Psi_0[Q_{\mathbf{k}r}, t] \propto \prod_{\mathbf{k}r} \exp\left(-\frac{1}{2}\omega Q_{\mathbf{k}r}^2\right) \exp\left(-i\frac{1}{2}\omega t\right), \quad (25)$$

where $\omega = (m^2 + k^2)^{1/2}$ and m is the mass associated with the field. (On expanding space the vacuum wave functional will reduce to this form in the short-wavelength limit.)

Let us assume that the quantum state of the field is indeed the vacuum state (25). Assuming for simplicity that the (putative) long-wavelength nonequilibrium modes are uncorrelated, we may then consider a hypothetical nonequilibrium vacuum with a distribution of the form

$$P_0[Q_{\mathbf{k}r}] \propto \prod_{\substack{\mathbf{k}r \\ (k > k_c)}} \exp(-\omega Q_{\mathbf{k}r}^2) \cdot \prod_{\substack{\mathbf{k}r \\ (k < k_c)}} \rho_{\mathbf{k}r}(Q_{\mathbf{k}r}), \quad (26)$$

where $\rho_{\mathbf{k}r}(Q_{\mathbf{k}r})$ is a general nonequilibrium distribution for the mode $\mathbf{k}r$ and the wavelength cutoff $2\pi/k_c$ is at least as large as the relevant lower bound (23) on λ^{vac} . The short wavelength modes ($k > k_c$) are in equilibrium while the long wavelength modes ($k < k_c$) are out of equilibrium. (The vacuum distribution P_0 is time independent because the de Broglie velocity field generated by (25) vanishes, $\dot{Q}_{\mathbf{k}r} = 0$, since the phase of the wave functional depends on t only.)

If the field Φ is now coupled to an external and classical electromagnetic field \mathbf{A}_{ext} , corresponding to a replacement $\nabla\Phi \rightarrow \nabla\Phi + ie\mathbf{A}_{\text{ext}}\Phi$ in the Hamiltonian, pairs of

oppositely charged bosons will be created from the vacuum.⁶ As in our discussion of inflaton decay, the probability distribution for the created particles originates from the initial probability distribution $P_0[Q_{\mathbf{k}r}]$ for the vacuum field Φ . (There are no other degrees of freedom varying over the ensemble, since the given classical field \mathbf{A}_{ext} is the same across the ensemble.) Clearly, if $P_0 \neq |\Psi_0|^2$ for long-wavelength modes, the final probability distribution for the created particles will necessarily carry traces of the initial nonequilibrium that was present in the vacuum. We could for example consider an interaction Hamiltonian $e^2 A_{\text{ext}}^2 \Phi^* \Phi$ and calculate the final particle distribution arising from a given initial nonequilibrium vacuum distribution of the form (26).

Similarly, processes of particle decay will be affected by the nonequilibrium vacuum. Consider, for example, the decay of a particle associated with a (bosonic or fermionic) field ψ that is coupled to Φ and to a third field χ . (For bosonic fields, the decay might be induced by an interaction Hamiltonian of the form $a\chi\Phi^2\psi$ where a is a coupling constant.) An initial state $|\mathbf{p}\rangle_\psi \otimes |0\rangle_\Phi \otimes |0\rangle_\chi$ —where $|\mathbf{p}\rangle_\psi$ is a single-particle state of momentum \mathbf{p} for the field ψ and $|0\rangle_\Phi, |0\rangle_\chi$ are respective vacua for the fields Φ and χ —may have a nonzero amplitude to make a transition⁷

$$|\mathbf{p}\rangle_\psi \otimes |0\rangle_\Phi \otimes |0\rangle_\chi \rightarrow |0\rangle_\psi \otimes |\mathbf{k}_1 \mathbf{k}_2\rangle_\Phi \otimes |\mathbf{p}'\rangle_\chi \quad (27)$$

to a final state containing two excitations of the field Φ and one excitation of χ . The final probability distribution for the outgoing particles will originate from the initial probability distribution for all the relevant (hidden-variable) degrees of freedom—which in this case consist of the relevant vacuum variables for Φ and χ together with the variables for the field ψ . (Again, if ψ is fermionic the associated hidden variables may consist of particle positions in the Dirac sea [43–45].) Because all these variables are coupled by the interaction, an initial nonequilibrium distribution (26) for a subset of them (that is, for the $Q_{\mathbf{k}r}$) will generally induce corrections to the Born rule in the final joint distribution for the collective variables and hence for the outgoing particles. Thus, for example, for gravitinos decaying in a

⁶The de Broglie-Bohm theory of a charged scalar field interacting with the electromagnetic field is discussed in Refs. [6,28].

⁷In a de Broglie-Bohm account, the apparent “collapse” of the quantum state as indicated by Eq. (27) is only an effective description. During a standard quantum process—such as a measurement, a scattering experiment, or general transition between eigenstates—an initial packet $\psi(q, 0)$ on configuration space evolves into a superposition $\psi(q, t) = \sum_n c_n \psi_n(q, t)$ of nonoverlapping packets $\psi_n(q, t)$. The final configuration $q(t)$ can occupy only one “branch”—say $\psi_i(q, t)$, corresponding to the i th “outcome”. The motion of $q(t)$ will subsequently be affected by $\psi_i(q, t)$ alone, resulting in an effective “collapse” of the wave function. The “empty” branches still exist but no longer affect the trajectory $q(t)$. (See, for example, Chapter 8 of Ref. [4].)

nonequilibrium vacuum we would expect the decay photons to carry traces of nonequilibrium in the probability distributions for their outgoing momenta and polarizations.

III. PERTURBATIVE TRANSFER OF NONEQUILIBRIUM

We now turn to some simple but illustrative field-theoretical models of the behavior of nonequilibrium systems. The first question that needs to be addressed is the perturbative transfer of nonequilibrium from one field to another. In this section we present a simple (bosonic) field-theoretical model that illustrates this process.

Suppose we have two Klein-Gordon fields ϕ_1 and ϕ_2 , confined inside a box of volume V with dimensions l_x, l_y , and l_z such that the fields are necessarily zero valued on the boundaries of the box. In consideration of these boundary conditions, we expand and quantize the fields in a set of standing waves as ($i = 1, 2$)

$$\phi_i(\mathbf{x}) = \sum_{\mathbf{k}} \frac{2^{3/2} q_{i\mathbf{k}}}{\sqrt{V}} \sin(k_x x) \sin(k_y y) \sin(k_z z), \quad (28)$$

with annihilation operators

$$a_{i\mathbf{k}} = \sqrt{\frac{\omega_{i\mathbf{k}}}{2}} \left(q_{i\mathbf{k}} + \frac{i}{\omega_{i\mathbf{k}}} p_{i\mathbf{k}} \right), \quad (29)$$

and a total Hamiltonian

$$H_0 = \sum_{\mathbf{k}} (\omega_{1\mathbf{k}} a_{1\mathbf{k}}^\dagger a_{1\mathbf{k}} + \omega_{2\mathbf{k}} a_{2\mathbf{k}}^\dagger a_{2\mathbf{k}}). \quad (30)$$

We have dropped the zero point energy, and $k_x = n\pi/l_x$ and similarly for y and z . The two fields are coupled by the interaction Hamiltonian

$$H_1 = g \int_V d^3x \phi_1(\mathbf{x}) \phi_2(\mathbf{x}) \quad (31)$$

$$= \frac{g}{2} \sum_{\mathbf{k}} \frac{1}{\sqrt{\omega_{1\mathbf{k}} \omega_{2\mathbf{k}}}} (a_{1\mathbf{k}} + a_{1\mathbf{k}}^\dagger) (a_{2\mathbf{k}} + a_{2\mathbf{k}}^\dagger), \quad (32)$$

where g is a coupling constant. If we suppose that at time $t = 0$ the system is in the free (unperturbed) eigenstate $|E_i\rangle$, the first order perturbative amplitude to transition to the state $|E_f\rangle$ is

$$d_f^{(1)}(t) = \langle f | H_1 | i \rangle \frac{e^{-iE_f t} - e^{-iE_i t}}{E_f - E_i}. \quad (33)$$

This will be damped for any E_f significantly different from E_i . We may exploit this fact by further insisting that

- (i) $l_x \gg l_y \gg l_z$, so that the lowest mode of each field is significantly lower than all others, and

(ii) the limit $m_2 \rightarrow m_1$ is taken, so that the lowest modes of ϕ_1 and ϕ_2 have the same unperturbed energy.

These conditions ensure that the system state in which field ϕ_1 has one particle occupying its lowest mode and the field ϕ_2 is a vacuum has identical unperturbed energy to the system state in which the individual field states are reversed. We shall denote these states $|1, 0\rangle$ and $|0, 1\rangle$ respectively. Since these states have identical unperturbed energies, the first order perturbative amplitudes (33) between the states is significantly amplified, whereas all others damped. This is the justification of the rotating wave approximation, familiar from quantum optics and cavity QED (see for instance Ref. [61]). Put simply, the states $|1, 0\rangle$ and $|0, 1\rangle$ are strongly coupled to each other and only very weakly coupled to any other state.

We make the rotating wave approximation by removing all terms in the Hamiltonian that would effect an evolution to states other than $|1, 0\rangle$ and $|0, 1\rangle$. This allows us to employ the effective Hamiltonian,

$$H_{\text{eff}} = \omega(a_1^\dagger a_1 + a_2^\dagger a_2) + \frac{g}{2\omega}(a_1 a_2^\dagger + a_2 a_1^\dagger). \quad (34)$$

We have suppressed the mode subscripts for simplicity. The approximate Schrödinger equation $H_{\text{eff}}|\psi\rangle = i\partial_t|\psi\rangle$, along with the initial condition $|\psi\rangle|_{t=0} = |1, 0\rangle$, yields the solution

$$|\psi\rangle = e^{-i\omega t} \left(\cos\left(\frac{gt}{2\omega}\right)|1, 0\rangle - i \sin\left(\frac{gt}{2\omega}\right)|0, 1\rangle \right). \quad (35)$$

The sine and cosine in Eq. (35) describe an oscillatory decay process in which the first type of particle is seen to decay into the second type, which promptly decays back. This type of flip-flopping between one type of particle and the other is functionally equivalent to vacuum-field Rabi oscillations in the Jaynes-Cummings model [61,62] of quantum optics and cavity QED wherein an exchange of energy occurs between an atom and a cavity mode of the electromagnetic field, perpetually creating a photon, then destroying it only to create it once more.⁸

To develop a de Broglie-Bohm description of this particle decay process, one needs to specify the

⁸From a field-theoretical viewpoint the quadratic interaction (31) may seem too trivial an example since the interaction may be removed by a linear transformation of the field variables. Such a transformation would not, however, negate the physical meaning of the original system. Our aim is to illustrate with a simple example how nonequilibrium may be passed from one type of field to another. We expect a similar passing of quantum non-equilibrium between fields to be caused by any reasonable interaction term. Our example is based on a model—widely used in quantum optics to study the interaction between a two-level atom and a single mode of the quantized electromagnetic field inside a cavity—that is simple enough to be tractable while at the same time providing a genuine field-theoretical account of energy transfer to and from a quantized field.

configuration of the system. For bosonic fields the canonical approach [3] is to use the Schrödinger representation with mode amplitudes as the configuration. In our case this is particularly simple; the state of any one system in an ensemble is described by the coordinates q_1 and q_2 , proportional to the amplitudes of the lowest (standing) mode of each field. In this representation the Hamiltonian is

$$H_{\text{eff}} = -\frac{1}{2}(\partial_{q_1}^2 + \partial_{q_2}^2) + \frac{1}{2}\omega^2(q_1^2 + q_2^2) - \omega + \frac{g}{2} \left(q_1 q_2 - \frac{1}{\omega^2} \partial_{q_1} \partial_{q_2} \right). \quad (36)$$

In the rotating wave approximation there are derivative terms in the interaction Hamiltonian. The de Broglie velocity fields associated with the Hamiltonian (36) may be derived in the standard way, and by using

$$\begin{aligned} \psi^* \partial_{q_1} \partial_{q_2} \psi - \psi \partial_{q_1} \partial_{q_2} \psi^* \\ = i \partial_{q_1} (|\psi|^2 \partial_{q_2} \text{Im} \ln \psi) + i \partial_{q_2} (|\psi|^2 \partial_{q_1} \text{Im} \ln \psi) \end{aligned} \quad (37)$$

(a special case of the general identity 2 of Ref. [36]). Writing $\psi = |\psi|e^{iS}$, the guidance equations may be expressed as

$$\begin{aligned} \dot{q}_1 &= \partial_{q_1} S + \frac{g}{2\omega^2} \partial_{q_2} S, \\ \dot{q}_2 &= \partial_{q_2} S + \frac{g}{2\omega^2} \partial_{q_1} S. \end{aligned} \quad (38)$$

For the particular state (35), these yield

$$\begin{aligned} \dot{q}_1 &= \frac{\frac{1}{2}(q_2 - \frac{g}{2\omega^2} q_1) \sin(\frac{gt}{2\omega})}{q_1^2 \cos^2(\frac{gt}{2\omega}) + q_2^2 \sin^2(\frac{gt}{2\omega})}, \\ \dot{q}_2 &= \frac{\frac{1}{2}(-q_1 + \frac{g}{2\omega^2} q_2) \sin(\frac{gt}{2\omega})}{q_1^2 \cos^2(\frac{gt}{2\omega}) + q_2^2 \sin^2(\frac{gt}{2\omega})}. \end{aligned} \quad (39)$$

The configuration $q(t) = (q_1(t), q_2(t))$ and velocity $\dot{q}(t) = (\dot{q}_1(t), \dot{q}_2(t))$ of a particular member of an ensemble evolving along a trajectory described by Eq. (39) has the properties $q(t) = q(t + 2\pi\omega/g)$, $\dot{q}(t) = \dot{q}(t + 2\pi\omega/g)$, $q(t) = q(-t)$, and $\dot{q}(t) = -\dot{q}(-t)$. The trajectories $q(t)$ are periodic, and halfway through their period backtrack along their original path.

Given the velocity field (39), we may integrate the continuity equation (2) to obtain the time evolution of an arbitrary distribution ρ . (Our numerical method is described in the Appendix.)

In Fig. 2 we compare the evolution of quantum non-equilibrium with that of equilibrium for the case $\omega = g = 1$. The decay from an initial product state $|1, 0\rangle$ to a final product state $|0, 1\rangle$ is seen in the (product) equilibrium distributions on the right-hand side of Fig. 2. We illustrate the transfer of nonequilibrium in the left-hand

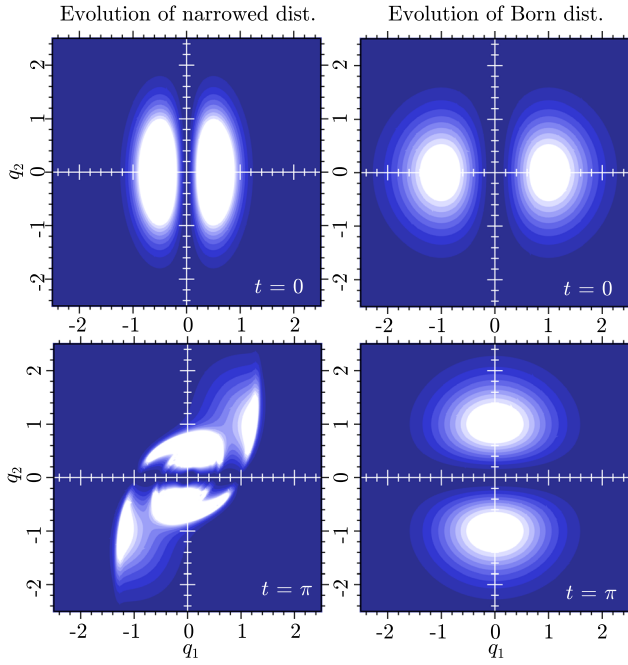


FIG. 2 (color online). The evolution of quantum equilibrium and nonequilibrium through the particle decay process described by state (35) and guidance equation (39). Initially state (35) is a product between an excited (one particle) state in q_1 and a ground (vacuum) state in q_2 . This is shown in the top right graph. As time passes, $t = 0 \rightarrow \pi$, the excited state in q_1 decays into exactly the same excited state in q_2 . At time $t = \pi$ the state (35) exists in another product state, except this time with excited and ground states switched between fields. This is shown in the bottom right graph. The evolution of a quantum nonequilibrium distribution is shown in the left column. Before the interaction takes place, quantum nonequilibrium exists only in the one particle state of the first field; it has been narrowed with respect to the equilibrium distribution. As time passes, the first field generates nonequilibrium in the second. At $t = \pi$, by standard quantum mechanics, the decay process is complete and there exists another product state. In contrast, the introduction of quantum nonequilibrium has created a distribution at $t = \pi$ that is correlated between q_1 and q_2 . The marginal distributions for the fields are shown in Fig. 3. (This figure takes $\omega = g = 1$.)

side of Fig. 2 for the case of an initial nonequilibrium that has simply been narrowed in q_1 (with respect to equilibrium). Hence only the first field is initially out of equilibrium. As time passes the distribution becomes correlated in q_1 and q_2 . At $t = \pi$, when according to standard quantum mechanics we should find another product state (corresponding to $|0, 1\rangle$), there exists a complicated overall nonequilibrium in (q_1, q_2) . The marginal distributions are shown in Fig. 3.

The evolution of nonequilibrium depends strongly on the particular values of ω and g , although in general we see two important properties of this evolution. Firstly it is apparent from Figs. 2 and 3 that nonequilibrium in the marginal distribution of the original particle state (or excited field) will generate nonequilibrium in its decay product.

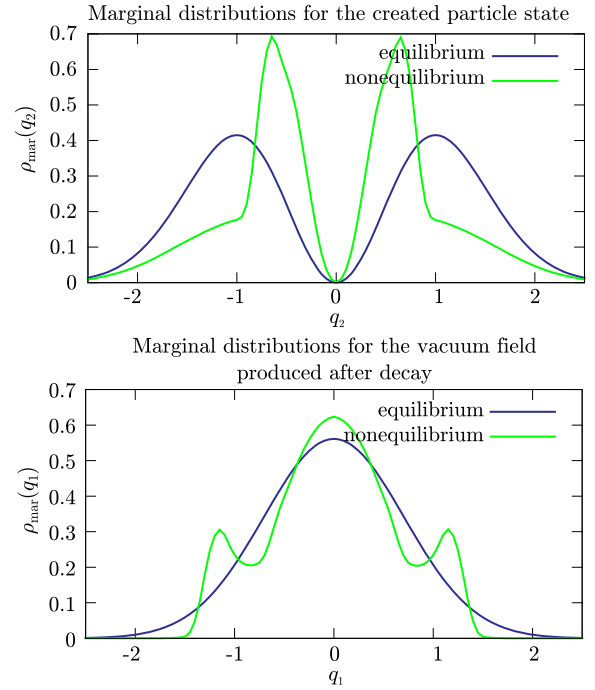


FIG. 3 (color online). The ensemble marginal distributions of the particle and vacuum state created at $t = \pi$ in the decay process shown in Fig. 2. The top graph shows the marginal distribution for the excited field $\rho_{\text{mar}}(q_2) = \int dq_1 \rho(q_1, q_2, t)|_{t=\pi}$. The bottom graph shows the nonequilibrium marginal distribution of the vacuum field $\rho_{\text{mar}}(q_1) = \int dq_2 \rho(q_1, q_2, t)|_{t=\pi}$, obtained after the original particle state has decayed.

Secondly, although the initial product state $|\psi\rangle|_{t=0} = |1, 0\rangle$ evolves into the product state $|0, 1\rangle$ at $t = \pi\omega/g$, the nonequilibrium distribution is correlated between the two fields. Such correlation could not exist in standard quantum mechanics.

IV. ENERGY MEASUREMENTS AND NONEQUILIBRIUM SPECTRA

In this section we focus on quantum-mechanical measurements of energy for elementary field-theoretical systems in nonequilibrium. As we have discussed, in this paper we restrict ourselves to simple models that may be taken to illustrate some of the basic phenomena that could occur.

The following analysis is presented for the electromagnetic field, partly because it provides a convenient illustrative model and partly because (as explained in Sec. II) we envisage the possibility of detecting decay photons produced by particles in nonequilibrium rather than the parent particles themselves. However, the analysis should apply equally well to other field theories.

A. Setup and effective wave function

We work in the Coulomb gauge, $\nabla \cdot \mathbf{A}(\mathbf{x}, t) = 0$, with the field expansion

$$\mathbf{A}(\mathbf{x}, t) = \sum_{\mathbf{k}'s'} [A_{\mathbf{k}'s'}(t)\mathbf{u}_{\mathbf{k}'s'}(\mathbf{x}) + A_{\mathbf{k}'s'}^*(t)\mathbf{u}_{\mathbf{k}'s'}^*(\mathbf{x})], \quad (40)$$

where the functions

$$\mathbf{u}_{\mathbf{k}'s'}(\mathbf{x}) = \frac{\boldsymbol{\varepsilon}_{\mathbf{k}'s'}}{\sqrt{2\varepsilon_0 V}} e^{i\mathbf{k}'\cdot\mathbf{x}} \quad (41)$$

and their complex conjugates define a basis for the function space. In expansion (40) and henceforth, summations over wave vectors are understood to extend over half the possible values of \mathbf{k}' . This is to avoid duplication of bases $\mathbf{u}_{\mathbf{k}'s'}$ with $\mathbf{u}_{-\mathbf{k}'s'}$. See for instance Ref. [63]. The primes are included for later convenience. This expansion allows one to write the energy of the electromagnetic field as

$$U = \frac{1}{2} \int_V d^3x \left(\varepsilon_0 \mathbf{E} \cdot \mathbf{E} + \frac{1}{\mu_0} \mathbf{B} \cdot \mathbf{B} \right) \quad (42)$$

$$= \sum_{\mathbf{k}'s'} \frac{1}{2} (\dot{A}_{\mathbf{k}'s'} \dot{A}_{\mathbf{k}'s'}^* + \omega_{\mathbf{k}'}^2 A_{\mathbf{k}'s'} A_{\mathbf{k}'s'}^*), \quad (43)$$

where $\omega_{\mathbf{k}'} = c|\mathbf{k}'|$. Equation (43) defines a decoupled set of complex harmonic oscillators of unit mass. We shall prefer instead to work with real variables and so we decompose $A_{\mathbf{k}'s'}$ into its real and imaginary parts

$$A_{\mathbf{k}'s'} = q_{\mathbf{k}'s'1} + iq_{\mathbf{k}'s'2}. \quad (44)$$

One may then write the free field Hamiltonian as

$$H_0 = \sum_{\mathbf{k}'s'r'} H_{\mathbf{k}'s'r'} \quad (45)$$

with $r' = 1, 2$, where

$$H_{\mathbf{k}'s'r'} = \frac{1}{2} (p_{\mathbf{k}'s'r'}^2 + \omega_{\mathbf{k}'}^2 q_{\mathbf{k}'s'r'}^2), \quad (46)$$

and where $p_{\mathbf{k}'s'r'}$ is the momentum conjugate of $q_{\mathbf{k}'s'r'}$.

Suppose we wish to perform a quantum energy measurement for a single mode of the field. We may follow the pilot-wave theory of ideal measurements described in Ref. [4]. The system is coupled to an apparatus pointer with position variable y . The interaction Hamiltonian H_I is taken to be of the form $g\hat{\omega}p_y$, where again g is a coupling constant and $\hat{\omega}$ is the operator corresponding to the observable to be measured. In our case we have

$$H_I = gH_{\mathbf{k}sr}p_y, \quad (47)$$

where p_y is the momentum conjugate to the pointer position y and where \mathbf{k} , s and r refer specifically to the field mode that is being measured. Including the free

Hamiltonian H_{app} for the apparatus, the total Hamiltonian is

$$H_{\text{tot}} = H_0 + H_{\text{app}} + H_I. \quad (48)$$

We assume an initial product state

$$\psi(0) = \psi_{\mathbf{k}sr}(q_{\mathbf{k}sr}, 0)\phi(y, 0)\chi(\mathcal{Q}, 0), \quad (49)$$

where $\psi_{\mathbf{k}sr}$ is the wave function for the mode in question, ϕ is the apparatus wave function and χ is a function of the rest of the field variables $\mathcal{Q} = \{q_{\mathbf{k}'s'r'} | (\mathbf{k}', s', r') \neq (\mathbf{k}, s, r)\}$. The function χ is left unspecified as there is no need to make assumptions concerning the state of the rest of the field. Now, since H_I and H_{app} commute with all the terms in H_0 that include \mathcal{Q} , under time evolution the χ function remains unentangled with the rest of the system while the apparatus and the mode being measured become entangled. We may then write

$$\psi(t) = \Psi(q_{\mathbf{k}sr}, y, t)\chi(\mathcal{Q}, t), \quad (50)$$

where

$$\begin{aligned} \Psi(q_{\mathbf{k}sr}, y, t) &= \exp[-i(H_{\mathbf{k}sr} + H_{\text{app}} + gH_{\mathbf{k}sr}p_y)t] \\ &\quad \times \psi_{\mathbf{k}sr}(q_{\mathbf{k}sr}, 0)\phi(y, 0), \\ \chi(\mathcal{Q}, t) &= \left[\prod_{(\mathbf{k}'s'r') \neq (\mathbf{k}sr)} \exp(-iH_{\mathbf{k}'s'r'}t) \right] \chi(\mathcal{Q}, 0). \end{aligned} \quad (51)$$

Since the system and apparatus remain unentangled with χ , the dynamics remain completely separate. We may concern ourselves only with $\Psi(q_{\mathbf{k}sr}, y, t)$ as an effective wave function. The velocity field in the $(q_{\mathbf{k}sr}, y)$ plane depends on the position in that plane but is independent of the position in \mathcal{Q} . We may then omit the $\mathbf{k}sr$ labels in $q_{\mathbf{k}sr}$ and $H_{\mathbf{k}sr}$, and the \mathbf{k} label in $\omega_{\mathbf{k}}$.

Let the measurement process begin at $t = 0$ when the coupling is switched on. As usual in the description of an ideal von Neumann measurement (see for example Ref. [4]), we take g to be so large that the free parts of the Hamiltonian may be neglected during the measurement. The system will then evolve according to the Schrödinger equation

$$(\partial_t + gH\partial_y)\Psi = 0. \quad (52)$$

Expanding Ψ in a basis $\psi_n(q)$ of energy states for the field mode, we have the solution

$$\Psi(q, y, t) = \sum_n c_n \phi(y - gE_n t) \psi_n(q), \quad (53)$$

where we choose ϕ and ψ_n to be real and $\sum_n |c_n|^2 = 1$. Equation (53) describes the measurement process. If the

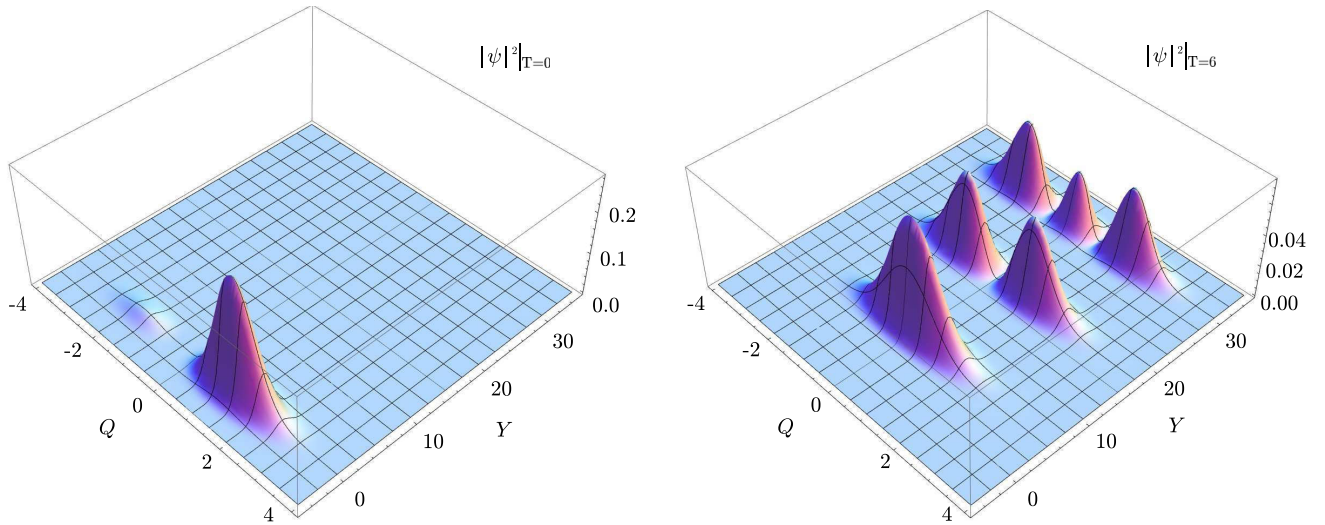


FIG. 4 (color online). Illustration of the energy measurement process, showing the evolution of the Born distribution into disjoint packets (for the case $c_0 = c_1 = c_2 = 1/\sqrt{3}$). The variables q , y and t have been replaced by the rescaled variables Q , Y and T defined in Sec. IV B. The initial pointer wave function is chosen to be a Gaussian centred on $Y = 0$. Initially the components of the total wave function overlap and interfere. As time passes each component moves in the Y direction with speed $2n + 1$. After some time the components no longer overlap and the experimenter may unambiguously read off the energy eigenvalue from the position of the pointer (Y coordinate).

initial system state is an energy eigenstate ($c_n = \delta_{mn}$ for some m), the pointer packet is translated with a speed proportional to the energy E_m of the eigenstate. By observing the displacement of the pointer after a time t , an experimenter may infer the energy of the field mode. If instead the field mode is initially in a superposition of energy states, the different components of the superposition will be translated at different speeds until such a time when they no longer overlap and thus do not interfere. An example of this evolution into nonoverlapping, noninterfering packets is shown in Fig. 4. At this time an experimenter could unambiguously read off an energy eigenvalue. The weightings $|c_n|^2$ in the superposition could be determined by readings over an ensemble.

B. Pointer packet and rescaling

For simplicity we choose the initial pointer wave function ϕ in Eq. (53) to be a Gaussian centred on $y = 0$,

$$\phi(y) = \sigma^{-1/2} (2\pi)^{-1/4} e^{-y^2/4\sigma^2}, \quad (54)$$

where σ^2 is the variance of $|\phi(y)|^2$.

It is convenient to introduce the rescaled parameters

$$Q = \sqrt{\omega}q, \quad Y = \frac{y}{\sigma}, \quad T = \frac{g\omega t}{2\sigma}. \quad (55)$$

The evolution of the wave function is then determined by the Schrödinger equation,

$$\partial_T \Psi = (\partial_Q^2 - Q^2) \partial_Y \Psi. \quad (56)$$

The general solution is

$$\begin{aligned} \Psi(Q, Y, T) = & \sum_n \frac{c_n}{\sqrt{\pi 2^{n+1/2} n!}} \\ & \times \exp \left[-\frac{1}{4} (Y - (2n+1)T)^2 \right] e^{-Q^2/2} H_n(Q), \end{aligned} \quad (57)$$

where $H_n(Q)$ are Hermite polynomials. [Equation (57) differs from Eq. (53) by a factor $\sigma^{1/2} \omega^{-1/4}$, to normalize the wave function in the rescaled configuration space.]

C. Continuity equation and guidance equations

From the Schrödinger equation (56), it is simple to arrive at

$$\partial_T |\Psi|^2 = \Psi^* \partial_Q^2 \partial_Y \Psi + \Psi \partial_Q^2 \partial_Y \Psi^* - \partial_Y (Q^2 |\Psi|^2). \quad (58)$$

From here we use the identity

$$\begin{aligned} & \Psi^* \partial_Q^2 \partial_Y \Psi + \Psi \partial_Q^2 \partial_Y \Psi^* \\ & \equiv \frac{1}{3} \partial_Q (2\Psi \partial_Q \partial_Y \Psi^* - \partial_Y \Psi \partial_Q \Psi^* \\ & \quad - \partial_Q \Psi \partial_Y \Psi^* + 2\Psi^* \partial_Q \partial_Y \Psi) \\ & \quad + \frac{1}{3} \partial_Y (\Psi \partial_Q^2 \Psi^* - \partial_Q \Psi \partial_Q \Psi^* + \Psi^* \partial_Q^2 \Psi). \end{aligned} \quad (59)$$

This, again, is a special case of the general identity 2 of [36]. The continuity equation is found to be

$$\begin{aligned} \partial_T |\Psi|^2 + \partial_Q \text{Re} \left(\frac{2}{3} \partial_Y \Psi \partial_Q \Psi^* - \frac{4}{3} \Psi^* \partial_Q \partial_Y \Psi \right) \\ + \partial_Y \text{Re} \left(\frac{1}{3} |\partial_Q \Psi|^2 - \frac{2}{3} \Psi^* \partial_Q^2 \Psi + Q^2 \right) = 0, \end{aligned} \quad (60)$$

from which we may deduce the de Broglie guidance equations

$$\partial_T Q = \text{Re} \left(-\frac{4}{3} \frac{\partial_Q \partial_Y \Psi}{\Psi} + \frac{2}{3} \frac{\partial_Y \Psi \partial_Q \Psi^*}{|\Psi|^2} \right), \quad (61)$$

$$\partial_T Y = \text{Re} \left(-\frac{2}{3} \frac{\partial_Q^2 \Psi}{\Psi} + \frac{1}{3} \frac{\partial_Q \Psi \partial_Q \Psi^*}{|\Psi|^2} \right) + Q^2. \quad (62)$$

The factor Q^2 in Eq. (62) will turn out to have the most predictable effect on the evolution of quantum nonequilibrium in Sec. IV E. Any individual system in which $|Q|$ is abnormally large will, at least to begin with, have an abnormally large pointer velocity. The Q^2 term originates from the potential term in $H_{ksr} = \frac{1}{2} p_{ksr}^2 + \frac{1}{2} \omega_k^2 q_{ksr}^2$.

In contrast with Sec. III, here we have chosen to retain the zero-point energy of the ksr mode. Since the pointer is coupled to the total energy of the ksr mode, this does affect the dynamics though only in a minor respect. Had we normal ordered Eq. (48), the pointer velocity Eq. (62) would have an extra additive term of -1 . In the state-specific expressions of Sec. IV D, normal ordering is equivalent to switching to a coordinate system moving in the $+Y$ direction at a (rescaled) velocity of 1, the velocity of the vacuum component in Eq. (57). Equivalently, one may use the coordinate transformation $Y \rightarrow Y' = Y - T$, which we shall indeed do in Sec. IV E 2.

D. Expressions for three examples

1. Vacuum

If the field mode being measured is in its vacuum state ($c_n = \delta_{n0}$), the evolution of the total wave function (57) and the associated velocity fields (61) and (62) are given by

$$\Psi = 2^{-\frac{1}{4}} \pi^{-\frac{1}{2}} \exp \left(-\frac{1}{2} Q^2 - \frac{1}{4} (Y - T)^2 \right), \quad (63)$$

$$\partial_T Q = \frac{1}{3} Q (T - Y), \quad (64)$$

$$\partial_T Y = \frac{2}{3} (1 + Q^2). \quad (65)$$

2. One particle state

If instead the field mode being measured contains one particle or excitation ($c_n = \delta_{n1}$), the relevant expressions are

$$\Psi = 2^{\frac{1}{4}} \pi^{-\frac{1}{2}} Q \exp \left(-\frac{1}{2} Q^2 - \frac{1}{4} (Y - 3T)^2 \right), \quad (66)$$

$$\partial_T Q = \frac{1}{3} (Y - 3T) \left(\frac{1}{Q} - Q \right), \quad (67)$$

$$\partial_T Y = \frac{1}{3} \frac{1}{Q^2} + \frac{4}{3} + \frac{2}{3} Q^2. \quad (68)$$

3. Initial superposition of vacuum and one particle state

For a superposition, the relative phases in the c_n 's will contribute to the dynamics. For a superposition of initial vacuum and one particle states, we take $c_0 = e^{i\theta}/\sqrt{2}$ and $c_1 = 1/\sqrt{2}$. Our expressions then become

$$\Psi = \left(\frac{e^{i\theta}}{\sqrt{2}} + Q e^{T(Y-2T)} \right) 2^{-\frac{1}{4}} \pi^{-\frac{1}{2}} e^{-\frac{1}{4}(Y-T)^2} \exp \left(-\frac{1}{2} Q^2 \right), \quad (69)$$

$$\begin{aligned} \partial_T Q = \text{Re} \left(\frac{-\frac{5}{3} T + \frac{2}{3} Q^2 T + \frac{1}{3} Y}{\frac{e^{i\theta}}{\sqrt{2}} e^{T(2T-Y)} + Q} \right) \\ + \frac{\frac{2}{3} Q T}{\left| \frac{e^{i\theta}}{\sqrt{2}} e^{T(2T-Y)} + Q \right|^2} - \frac{1}{3} (Y - T) Q, \end{aligned} \quad (70)$$

$$\begin{aligned} \partial_T Y = \text{Re} \left[\frac{\frac{2}{3} Q}{\frac{e^{i\theta}}{\sqrt{2}} e^{T(2T-Y)} + Q} \right] + \frac{\frac{1}{3}}{\left| \frac{e^{i\theta}}{\sqrt{2}} e^{T(2T-Y)} + Q \right|^2} \\ + \frac{2}{3} (Q^2 + 1). \end{aligned} \quad (71)$$

E. Results for nonequilibrium energy measurements

We will now consider outcomes of quantum energy measurements for nonequilibrium field modes. Like many features of quantum mechanics, the usual statistical energy conservation law emerges in equilibrium. But for nonequilibrium states there is no generally useful notion of energy conservation.⁹

We may consider a parameterization of nonequilibrium that simply varies the width of the Born distribution (as discussed in Sec. II A for primordial perturbations). Our initial ρ is written

$$\rho(Q, Y, 0) = \frac{1}{w} |\Psi(Q/w, Y, 0)|^2, \quad (72)$$

where w is a widening parameter equal to the initial standard deviation of ρ relative to $|\Psi|^2$,

⁹The fundamental dynamical equation (1) is first order in time and has no naturally conserved energy. When rewritten in second order form there appears a time-dependent ‘‘quantum potential’’ that acts as an effective external energy source [4].

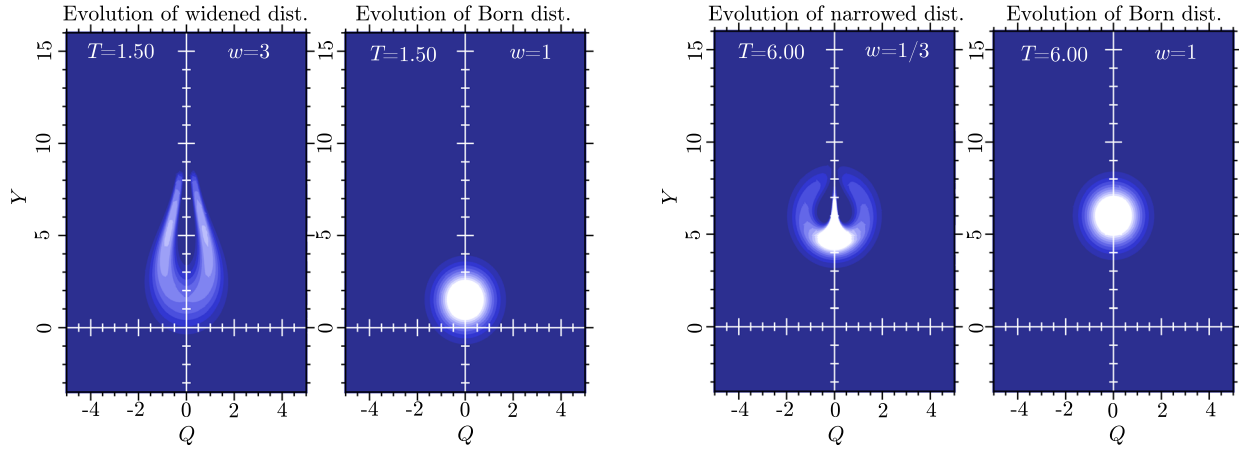


FIG. 5 (color online). The evolution of vacuum nonequilibria under an energy measurement process (as simulated by the code discussed in the Appendix). On the left is a snapshot of the evolution of a widened initial ρ with $w = 3$, taken at $T = 1.50$. The tails of ρ evolve quickly to large Y and small Q . These tails are evident in the marginal distribution for Y shown in Fig. 6. On the right is the same simulation except narrowed by a factor $w = 1/3$, and taken at $T = 6.00$. In this case ρ remains in what might loosely be deemed the support of $|\Psi|^2$, though displaying internal structure. The narrowed ρ initially lags behind the Born distribution, before getting swept outwards and upwards, creating a double-bump in the pointer marginal distribution. Note that the equilibrium pointer distribution undergoes an upward displacement to indicate the zero-point energy of the vacuum mode.

$$w = \frac{\sigma_\rho}{\sigma_{|\Psi|^2}} \Big|_{t=0}. \quad (73)$$

[Comparing with Eq. (7), we would have $w = \sqrt{\xi}$ for primordial perturbations.]

1. Short-time measurement of vacuum modes

In Fig. 5 we show the short-time behavior of widened and narrowed nonequilibrium distributions ρ under the

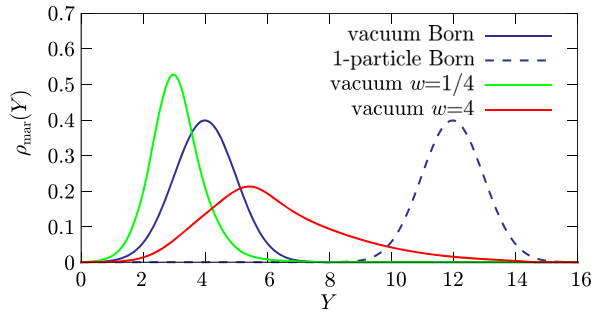


FIG. 6 (color online). Marginal pointer distributions $\rho_{\text{mar}}(Y)$ under the energy measurement of vacuum mode nonequilibria at $T = 4$. (For comparison we also show the Born pointer marginals for the vacuum and one-particle cases.) For the widened vacuum mode ($w = 4$), there is a significant probability of “detecting a particle” (that is, an excited state) in the vacuum mode. For this case there also exists a significant probability of finding the pointer around $Y = 8$ (which for all practical purposes would be impossible without nonequilibrium for any initial superposition). For the narrowed nonequilibrium ($w = 1/4$), the pointer distribution lags behind the Born pointer distribution initially. As time progresses, ρ will get swept outwards and upwards (cf. the right-hand side of Fig. 5), creating a double-bump in the pointer distribution.

energy measurement of a vacuum mode. As the Q^2 term in the Y velocity (65) dominates for any $|Q|_{t=0} > 1$, widened distributions show more initial movement of the pointer. The tails of widened distributions “flick” forwards and inwards, and then seem to linger. It is at this time that the pointer position could indicate the detection of an excited state (or particle) for the vacuum, or even occupy a position disallowed by standard quantum mechanics for any initial superposition of energy states (see Fig. 6). The closer the tails get to the Q -axis, the slower the pointer travels. Once inside $|Q| < 1/\sqrt{3}$, the tails move slower than the Born distribution (which eventually catches up). So although the widened distribution may produce the most dramatic deviations from standard quantum mechanics, the deviations are short-lived and any measuring device would need to make its measurement before the tails recede.

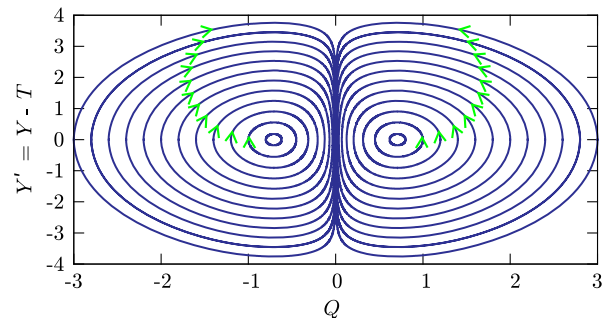


FIG. 7 (color online). Above, a selection of the trajectories for the measurement of a vacuum mode (with normal ordering). The velocity field is time independent, resulting in periodic orbits around $(\pm\sqrt{1/2}, 0)$. Numerical simulations show that the pointer marginals converge to stationary nonequilibrium distributions characteristic of the initial nonequilibrium state (see Fig. 8).

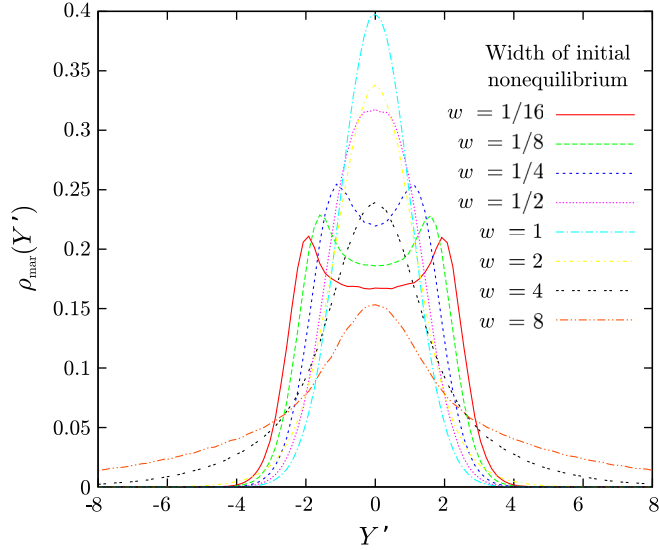


FIG. 8 (color online). Characteristic stationary pointer marginals $\rho_{\text{mar}}(Y')$ for energy measurement of nonequilibrium vacuum modes in the large T or large g approximation. In this regime, initial nonequilibrium in the field mode will produce a corresponding stationary nonequilibrium for the pointer. Field modes with larger spread produce pointer marginals with larger spread. Field modes with smaller spread form pointer marginals with central depressions.

In contrast, the narrowed distribution shows less dramatic behavior. It recedes slowly to the back of the Born distribution, and then some is swept out, up and around the Born distribution (see the right-hand side of Fig. 5). The pointer stays roughly where one would expect it to from standard quantum mechanics.

If one were to perform an ensemble of similar preparations and measurements, recording the position of the pointer in each, one would find the marginal distribution $\rho_{\text{mar}}(Y)$. The marginal distributions for $w = 1/4, 1$ and 4

are shown at $T = 4$ in Fig. 6. Any deviation that this distribution shows from the marginal Born distribution would of course be indicative of quantum nonequilibrium.

2. Long-time (large g) measurement of vacuum modes

Let us discuss a second measurement regime, which may be thought of as valid for large T and/or [since $T = g\omega t/(2\sigma)$] large g .

To aid analysis, we shall continue as if we had normal ordered the Hamiltonian (48). This, as mentioned in Sec. IV C, is equivalent to switching to the “reference frame” of the Born distribution with $Y \rightarrow Y' = Y - T$. Under normal ordering the wave function and guidance equations become

$$\Psi = 2^{-\frac{1}{4}}\pi^{-\frac{1}{2}}\exp\left(-\frac{1}{2}Q^2 - \frac{1}{4}Y'^2\right), \quad (74)$$

$$\partial_T Q = -\frac{1}{3}QY', \quad (75)$$

$$\partial_T Y' = \frac{2}{3}Q^2 - \frac{1}{3}. \quad (76)$$

The guidance equations are now time-independent and conserve a stationary Born distribution. The trajectories are periodic. A selection of the trajectories produced by Eqs. (75) and (76) are shown in Fig. 7. The trajectories do not pass the line $Q = 0$, and so we cannot find relaxation to the Born distribution for any initial ρ asymmetric in Q .

Our numerical simulations indicate that any nonequilibrium in the vacuum mode will, in the large T or large g limit, produce a corresponding stationary nonequilibrium in the pointer distribution. Furthermore, from this pointer distribution, numerical simulations could deduce the initial

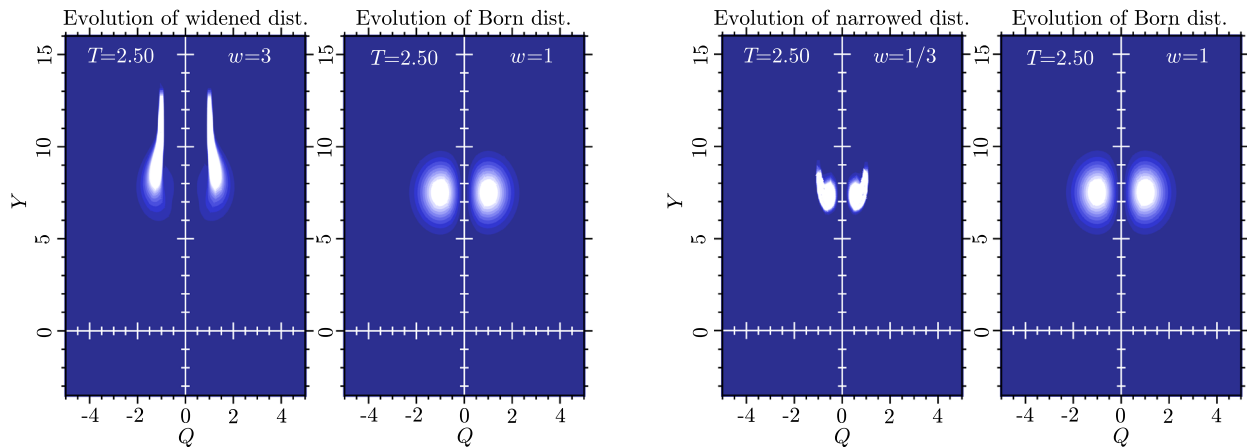


FIG. 9 (color online). The evolution of nonequilibria under energy measurement of single-particle states. On the left, a widened ($w = 3$) nonequilibrium distribution; on the right, a narrowed ($w = 1/3$) nonequilibrium distribution. The Born distribution, shown for comparison in each case, moves at a rescaled speed of $dY/dT = 3$ (although individual de Broglie trajectories have variable speeds). Pointer marginal distributions for this process are shown in Fig. 10.

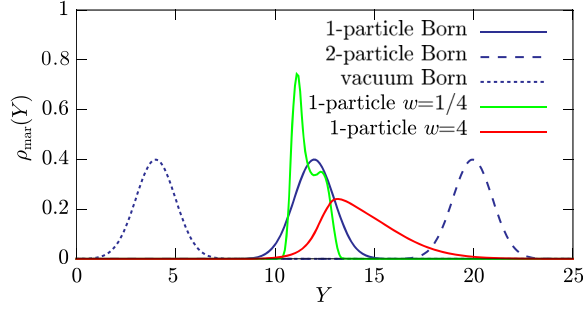


FIG. 10 (color online). Marginal pointer distributions $\rho_{\text{mar}}(Y)$ under energy measurement of one particle state nonequilibrium at time $T = 4$. (For comparison we also show the Born pointer marginals for the vacuum, one-particle and two-particle cases.) The widened nonequilibrium ($w = 4$) shows a significant probability of detecting two excitations (or “particles”) instead of one, and again there is a significant probability of finding the pointer around $Y = 16$ (a position disallowed by standard quantum mechanics for any initial superposition). As in the case of the vacuum mode measurement, the narrowed nonequilibrium ($w = 1/4$) will be distinguished only by its internal structure. The tendency to form a double-bump in the pointer distribution is also seen in this case.

nonequilibrium in the vacuum mode. Our simulations show that this limit will be reached at $T \sim 120$ for $1/8 < w < 8$.

Eight such stationary pointer marginals are displayed in Fig. 8. These are found under the measurement of nonequilibrium vacuum modes described by width parameters ranging from $w = 1/16$ to 8. Nonequilibrium modes that are wider than equilibrium make the spread in the pointer position correspondingly wider. In contrast, for the measurement of nonequilibrium vacuum modes that are narrower than equilibrium, the pointer marginal forms a central depression whilst staying in the same region. Measurements of the pointer over an ensemble would be

enough to deduce the character of the initial nonequilibrium for each case.

3. Measurement of a single particle state

Under the energy measurement process, the effective wave function becomes Eq. (66) and the trajectories satisfy the guidance equations (67) and (68). The Born distribution evolves in the Y direction at a rescaled velocity $dY/dT = 3$. Since now the Y velocity [Eq. (68)] has terms proportional to Q^2 and $1/Q^2$, we might expect some increased pointer movement both for the widened and narrowed nonequilibrium cases. In fact, our simulations show that a narrowed distribution yields relatively less pointer movement than the widened distribution (as we had for the case of the vacuum). Plots of the evolution of $\rho(Q, Y, T)$ are shown in Fig. 9, and marginal pointer distributions are shown in Fig. 10. As in the case of the vacuum mode measurement, there is a significant probability of detecting an extra excitation or of finding the pointer in a position disallowed by standard quantum mechanics for any superposition being measured.

4. Measurement of a superposition

Quantum nonequilibrium would in general cause anomalous results for the spectra of energy measurements. To illustrate this, we take the simple example of an equal superposition of vacuum and one-particle states. Quantum mechanically, an experimenter would observe a 50% probability of detecting a particle. We take $c_0 = e^{i\theta}/\sqrt{2}$ and $c_1 = 1/\sqrt{2}$, with the wave function and velocity fields specified in Eqs. (69–71). The dynamics of the measurement depends strongly on the initial relative phase θ of the superposition. This is seen in Fig. 11, where we show the time evolution of joint distributions $\rho(Q, Y, T)$. Examples

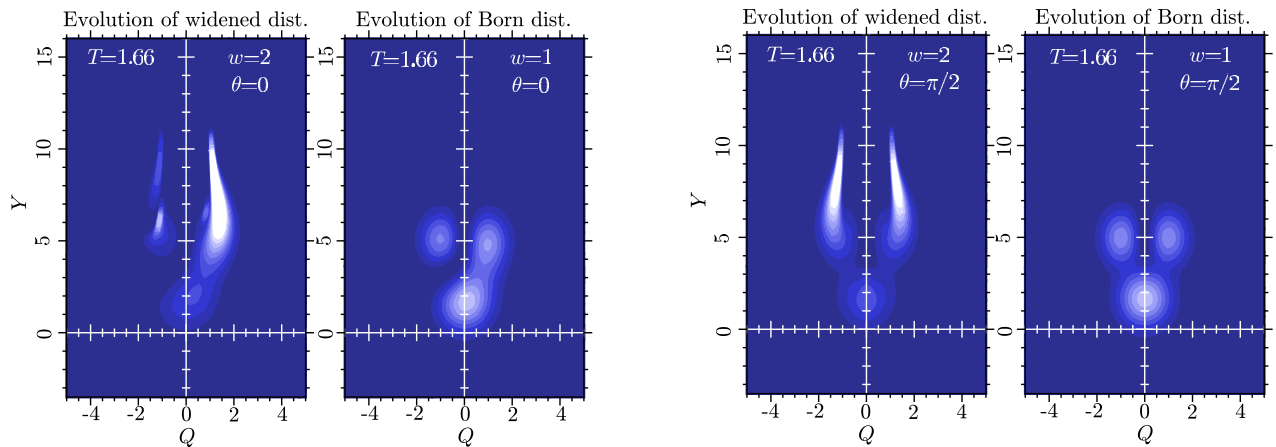


FIG. 11 (color online). Evolution of joint distributions $\rho(Q, Y, T)$ under energy measurements of a nonequilibrium field mode in a superposition of a vacuum and a one-particle state with $c_0 = e^{i\theta}/\sqrt{2}$ and $c_1 = 1/\sqrt{2}$ [Eq. (69)]. On the left we have taken $\theta = 0$. On the right we have taken $\theta = \pi/2$. Both cases have widened distributions with $w = 2$, and snapshots are taken at $T = 1.66$. (For comparison, Born distributions are also shown in both cases.)

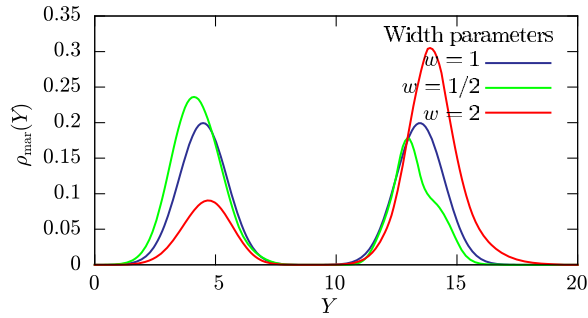


FIG. 12 (color online). Marginal pointer distributions $\rho_{\text{mar}}(Y)$ for $c_0 = c_1 = 1/\sqrt{2}$ and $w = 1/2, 1, 2$, taken at $T = 4.5$. Non-equilibrium is seen to cause anomalous spectra as observed by an experimenter. Similar results are obtained for other relative phases.

of the marginal pointer distributions produced in the energy measurement process are shown in Fig. 12. After about $T = 3.5$, all marginal pointer distributions display two distinct areas of support, meaning that an experimenter would unambiguously obtain either $\frac{1}{2}\omega$ or $\frac{3}{2}\omega$ in each individual energy measurement, regardless of whether nonequilibrium is present or not. However, a widened nonequilibrium distribution would cause a larger probability of obtaining the outcome $\frac{3}{2}\omega_k$ (“detecting a particle”), while a narrowed nonequilibrium would cause

the opposite effect. Although the trajectories are strongly dependent on the initial phase, the marginal pointer distributions are only weakly dependent on this.

In practice, one might not know the initial relative phase of the superposition. To make contact with what an experimenter might actually measure (albeit in the context of our simplified field-theoretical model), we have taken an average over ten phases: $\theta = 2\pi n/10, n = 0, 1, \dots, 9$. We run each simulation up to time $T = 4.5$ and calculate the proportion of the distribution ρ that lies beyond $Y = 9.0$. This is the probability of observing an excitation, whilst the proportion of ρ before $Y = 9.0$ is the probability of observing the vacuum. (These numbers are clear from Fig. 12.) Figure 13 illustrates the results of this averaging process for 20 separate width parameters w . We find a remarkable correlation. For example, for nonequilibrium close to the Born distribution, widening the distribution will proportionally increase the ensemble probability of “detecting a particle”. Clearly, nonequilibrium would generate an incorrect energy spectrum.

V. CONCLUSION

We have considered the possibility that our universe contains quantum nonequilibrium systems—in effect a new form or phase of matter (including the vacuum) that violates the Born probability rule and which is theoretically

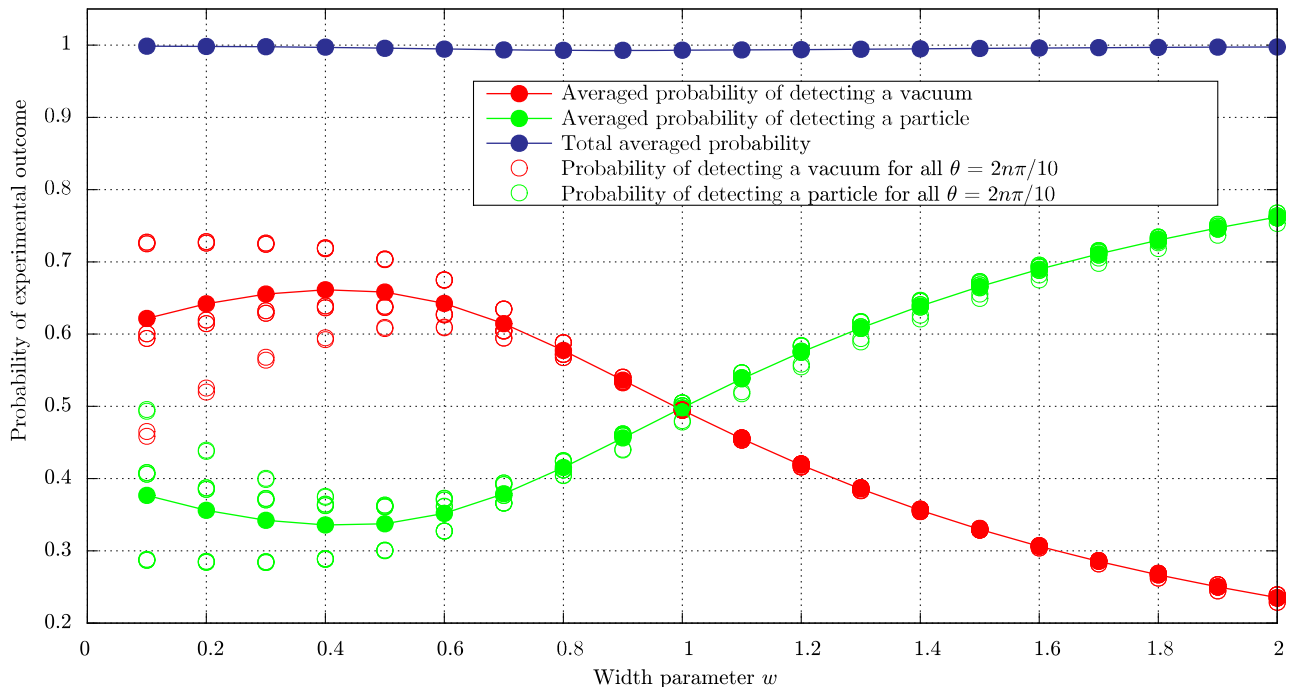


FIG. 13 (color online). Ensemble probabilities of energy measurements for an equal superposition of particle and vacuum states as affected by quantum nonequilibrium of varying width w (with results averaged over the relative phase θ in the superposition). As $|c_0| = |c_1| = 1/\sqrt{2}$, there should be a 50% probability of detecting a particle. However, widened nonequilibria give probabilities larger than 50% for particle detection, while narrowed nonequilibria give probabilities less than 50% for particle detection when averaged over θ . (Hollow markers represent results for individual relative phases θ , whilst solid markers represent averages over $\theta = 2n\pi/10, n = 1, 2, \dots, 10$. Dependence on the relative phase is seen to affect the outcomes only for $w \lesssim 1$.)

possible in the de Broglie-Bohm formulation of quantum theory. While the practical likelihood of detecting such systems remains difficult to evaluate, we have argued that at least in principle they could exist today as relics from the very early Universe. We have provided simple field-theoretical models illustrating the effects of quantum nonequilibrium in a particle-physics context. In particular, we have seen that quantum nonequilibrium would generate anomalous spectra for standard measurements of energy, as well as generating corrections to particle-physics processes generally.

The possibility of detecting relic nonequilibrium systems today depends on uncertain features of high-energy physics and cosmology. Dark matter, which is thought to make up approximately 25% of the mass-energy of the Universe, may consist of relic particles (such as gravitinos) that were created in the very early Universe and which have propagated essentially freely ever since. (For reviews see, for example, Refs. [54,64].) As we have seen, such particles are plausible candidates for carriers of primordial quantum nonequilibrium, and we expect that particle-physics processes involving them—for example, decay or annihilation—would display energetic anomalies.

On the experimental front, an especially promising development would be the detection of photons from dark matter decay or annihilation. These are expected to form a sharp spectral line, probably in the gamma-ray region. Recent interest has focused on reports of a sharp line from the Galactic center at ~ 130 GeV in data from the *Fermi* Large Area Telescope (LAT) [65,66]. While the line might be a dark matter signal, its significance (and even its existence) is controversial. The line could be caused by a number of scenarios involving dark matter annihilations [67]. It might also be due to decaying dark matter [68], for example the decay of relic gravitinos [69,70]. (In a supersymmetric extension of the Standard Model with violation of R-parity, the gravitino is unstable and can decay into a photon and a neutrino [71].) On the other hand, a recent analysis of the data by the *Fermi*-LAT team casts doubt on the interpretation of the line as a real dark matter signal [72].

Should dark matter consist (if only partially) of relic nonequilibrium systems, we may expect to find energetic anomalies for decay and annihilation processes. However, to distinguish these from more conventional effects would require more detailed modelling than we have provided here. There is also the question of whether the anomalies are likely to be large enough to observe in practice. These are matters for future work.

In principle, it would be of interest to test dark matter decay photons for possible deviations from the Born rule (perhaps via their polarization probabilities [35]). We have seen that simple perturbative couplings will transfer nonequilibrium from one field to another, leading us to expect that in general a decaying nonequilibrium particle will transfer nonequilibrium to its decay products. Another open

question, however, is the degree to which the nonequilibrium might be degraded during this process. In a realistic model of a particle decay we might expect some degree of relaxation. It would be useful to study this in pilot-wave models of specific decay processes.

As a general point of principle, one might also be concerned that in the scenario discussed in this paper the probability distribution for delocalized field modes in the early Universe—where the probability distribution is presumably defined for a theoretical ensemble—appears to have measurable implications for decay particles in our one Universe. How can this be? A similar point arises in the standard account of how the power spectrum for primordial perturbations has measurable implications for our one CMB sky. In inflationary theory, the probability distribution for a single mode $\phi_{\mathbf{k}}$ of the inflaton field does have measurable implications in our single Universe. As we discussed in Sec. II A, the variance $\langle |\phi_{\mathbf{k}}|^2 \rangle$ of the primordial inflaton distribution appears in the power spectrum $\mathcal{P}_{\mathcal{R}}(k) \propto \langle |\phi_{\mathbf{k}}|^2 \rangle$ for primordial curvature perturbations $\mathcal{R}_{\mathbf{k}} \propto \phi_{\mathbf{k}}$ at wave number k . The power spectrum $\mathcal{P}_{\mathcal{R}}(k)$ in turn appears in the angular power spectrum C_l [Eq. (8)], which may be accurately measured for our single CMB sky provided l is not too small. In the standard analysis it is assumed that the underlying “theoretical ensemble” of universes is statistically isotropic, which implies that the ensemble variance $C_l \equiv \langle |a_{lm}|^2 \rangle$ is independent of m —where a_{lm} are the harmonic coefficients for the observed temperature anisotropy. We then in effect have $2l + 1$ measured quantities a_{lm} with the same theoretical variance. Provided l is sufficiently large, one can perform meaningful statistical tests for our single CMB sky and compare with theoretical predictions for C_l . Statistical homogeneity also plays a role in relating the C_l 's for a single sky to the power spectrum $\mathcal{P}_{\mathcal{R}}(k)$ for the theoretical ensemble [18,25]. To understand how the theoretical ensemble probability has measurable implications in a single universe, it is common to speak of the CMB sky as divided up into patches—thereby providing an effective ensemble in one sky. This works if l is sufficiently large, so that the patches are sufficiently small in angular scale and therefore sufficiently numerous. Similar reasoning applies to particles (or field excitations) generated by inflaton decay. In this context it is important to note that realistic particle states, as observed for example in the laboratory, are represented by field modes defined with respect to finite spatial volumes V . Almost all of the particles in our Universe were created by inflaton decay, and in practice their states are in effect defined with respect to finite spatial regions. By measuring particle excitations in different spatial regions, it is possible to gather statistics for outcomes of (for example) energy measurements. (One might also consider a time ensemble in one region, but a space ensemble seems more relevant in the case of relic decay particles.) The resulting statistical distribution of outcomes for the decay particles will depend

on the original probability distribution for the decaying inflaton field—just as the statistics for patches of the CMB sky depend on the probability distribution for the inflaton during the inflationary era. A full account would require an analysis of inflaton decay more precise than is currently available. In particular, one would like to understand how this process yields particle states that are confined to finite spatial regions. It is generally understood that the decay products form as excitations of sub-Hubble modes, with wave functions confined to sub-Hubble distances. Depending on the details, this can correspond to relatively small spatial distances today. Of course, particle wave packets will also spread out since their creation, but still we may expect them to occupy finite spatial regions. Further elaboration of this point lies outside the scope of this paper.

Even if there exist localised sources or spatial regions containing particles in a state of quantum nonequilibrium, it might be difficult in practice to locate those regions. In particular, if a given detector registers particles belonging to different regions without distinguishing between them, then it is possible that even if nonequilibrium is present in the individual regions it will not be visible in the data because of averaging effects. How one might guard against this in practice remains to be studied.

Finally, we have seen that the likelihood of nonequilibrium surviving until today for relic particles depends on the fact that a nonequilibrium residue can exist in the long-time limit for systems containing a small number of superposed energy states [38]. While this may certainly occur in principle, its detailed implementation for realistic scenarios requires further study. On the other hand, no such question arises in our scenario for relic nonequilibrium vacuum modes, since the simplicity of vacuum wave functionals guarantees that further relaxation will not occur at late times. Long-wavelength vacuum modes may be carriers of primordial quantum nonequilibrium, untouched by the violent astrophysical history that (according to our hypotheses) long ago drove the matter we see to the quantum equilibrium state that we observe today. It remains to be seen if, in realistic scenarios, the effects on particle-physics processes taking place in a nonequilibrium vacuum could be large enough to be detectable.

ACKNOWLEDGMENTS

This research was funded jointly by the John Templeton Foundation and Clemson University.

APPENDIX: NUMERICAL METHODOLOGY

Most studies of relaxation in de Broglie-Bohm theory have used the backtracking method of Ref. [8] (see for instance [8,10,11,21]). This method uses the fact that the ratio $f = \rho(\mathbf{x}, t)/|\psi(\mathbf{x}, t)|^2$ is conserved along trajectories. A uniform grid of final positions is evolved backwards from the final time t_f to the initial time t_i . The final distribution is constructed from the conserved function f . Although this method has been successful in producing accurate results, it has the disadvantage that backtracking to t_i must be carried out for each desired final time t_f .

We have instead chosen to integrate the continuity Eq. (2) directly using a finite-volume method. The method used is a variant of the corner transport upwind method detailed in Secs. 20.5 and 20.6 of [73], modified so as to apply to the conservative form of the advection equation. This algorithm has the advantage that different “high resolution limiters” may be switched off and on with ease, so that one may compare results. (We use a monotonized central limiter throughout.) The main disadvantage of this approach is a consequence of the velocity field (61) and (62) diverging at nodes (where $|\psi| \rightarrow 0$). Since such an algorithm is required to satisfy a Courant-Friedrichs-Lewy condition to maintain stability, without velocity field smoothing the algorithm is inherently unstable. We have found that a simple way to implement a smoothing is to impose a maximum absolute value on the velocities. The maximum is taken throughout to be $1/10^{\text{th}}$ of the ratio of grid spacing to time step.

We have found that the finite-volume method is less efficient than the backtracking method over larger time scales. In fact, the long-time simulations shown in Fig. 8 were produced using a fifth-order Runge-Kutta algorithm to evolve trajectories directly. However for short time scales—the prime focus of this work—the finite-volume method is a useful tool.

[1] L. de Broglie, in *Électrons et Photons: Rapports et Discussions du Cinquième Conseil de Physique* (Gauthier-Villars, Paris, 1928); G. Bacciagaluppi and A. Valentini, *Quantum Theory at the Crossroads: Reconsidering the 1927 Solvay Conference* (Cambridge University Press, Cambridge, 2009).

[2] D. Bohm, *Phys. Rev.* **85**, 166 (1952).

[3] D. Bohm, *Phys. Rev.* **85**, 180 (1952).

[4] P. R. Holland, *The Quantum Theory of Motion: an Account of the de Broglie-Bohm Causal Interpretation of Quantum Mechanics* (Cambridge University Press, Cambridge, 1993).

[5] A. Valentini, *Phys. Lett. A* **156**, 5 (1991).

[6] A. Valentini, Ph.D. thesis, International School for Advanced Studies, Trieste, Italy, 1992, <http://urania.sissa.it/xmlui/handle/1963/5424>.

- [7] A. Valentini, in *Chance in Physics: Foundations and Perspectives*, edited by J. Bricmont *et al.* (Springer, Berlin, 2001), p. 165.
- [8] A. Valentini and H. Westman, *Proc. R. Soc. A* **461**, 253 (2005).
- [9] C. Efthymiopoulos and G. Contopoulos, *J. Phys. A* **39**, 1819 (2006).
- [10] M. D. Towler, N. J. Russell, and A. Valentini, *Proc. R. Soc. A* **468**, 990 (2012).
- [11] S. Colin, *Proc. R. Soc. A* **468**, 1116 (2012).
- [12] A. Valentini, *Phys. Lett. A* **158**, 1 (1991).
- [13] A. Valentini, in *Bohmian Mechanics and Quantum Theory: An Appraisal*, edited by J. T. Cushing, A. Fine, and S. Goldstein (Kluwer, Dordrecht, 1996).
- [14] A. Valentini, *Pramana J. Phys.* **59**, 269 (2002).
- [15] A. Valentini, *J. Phys. A* **40**, 3285 (2007).
- [16] A. Valentini, [arXiv:0804.4656](https://arxiv.org/abs/0804.4656).
- [17] A. Valentini, *Phys. World* **22N11**, 32 (2009).
- [18] A. Valentini, *Phys. Rev. D* **82**, 063513 (2010).
- [19] A. Valentini, in *Many Worlds? Everett, Quantum Theory, & Reality*, edited by S. Saunders *et al.* (Oxford University Press, Oxford, 2010).
- [20] P. Pearle and A. Valentini, in *Encyclopaedia of Mathematical Physics*, edited by J.-P. Francoise *et al.* (Elsevier, North-Holland, 2006).
- [21] S. Colin and A. Valentini, *Phys. Rev. D* **88**, 103515 (2013).
- [22] S. Colin and A. Valentini, *Phys. Rev. D* **92**, 043520 (2015).
- [23] P. Peter, A. Valentini, and S. D. P. Viteni, (to be published).
- [24] A. R. Liddle and D. H. Lyth, *Cosmological Inflation and Large-Scale Structure* (Cambridge University Press, Cambridge, 2000).
- [25] V. Mukhanov, *Physical Foundations of Cosmology* (Cambridge University Press, Cambridge, 2005).
- [26] S. Weinberg, *Cosmology* (Oxford University Press, Oxford, 2008).
- [27] P. Peter and J.-P. Uzan, *Primordial Cosmology* (Oxford University Press, Oxford, 2009).
- [28] A. Valentini, *Hidden Variables in Modern Physics and Beyond* (Cambridge University Press, Cambridge, forthcoming).
- [29] A. Vilenkin and L. H. Ford, *Phys. Rev. D* **26**, 1231 (1982).
- [30] A. D. Linde, *Phys. Lett.* **116B**, 335 (1982).
- [31] A. A. Starobinsky, *Phys. Lett.* **117B**, 175 (1982).
- [32] B. A. Powell and W. H. Kinney, *Phys. Rev. D* **76**, 063512 (2007).
- [33] I.-C. Wang and K.-W. Ng, *Phys. Rev. D* **77**, 083501 (2008).
- [34] P. A. R. Ade *et al.* (Planck Collaboration), *Astron. Astrophys.* **571**, A15 (2014).
- [35] A. Valentini, *Phys. Lett. A* **332**, 187 (2004).
- [36] W. Struyve and A. Valentini, *J. Phys. A* **42**, 035301 (2009).
- [37] A. Valentini, in *Einstein, Relativity and Absolute Simultaneity*, edited by W. L. Craig and Q. Smith (Routledge, London, 2008).
- [38] E. Abraham, S. Colin, and A. Valentini, *J. Phys. A* **47**, 395306 (2014).
- [39] A. Valentini, [arXiv:hep-th/0407032](https://arxiv.org/abs/hep-th/0407032).
- [40] R. H. Brandenberger and J. Martin, *Mod. Phys. Lett. A* **16**, 999 (2001).
- [41] J. Martin and R. H. Brandenberger, *Phys. Rev. D* **63**, 123501 (2001).
- [42] R. H. Brandenberger and J. Martin, *Classical Quantum Gravity* **30**, 113001 (2013).
- [43] D. Bohm and B. J. Hiley, *The Undivided Universe: an Ontological Interpretation of Quantum Theory* (Routledge, London, 1993).
- [44] S. Colin, *Phys. Lett. A* **317**, 349 (2003).
- [45] S. Colin and W. Struyve, *J. Phys. A* **40**, 7309 (2007).
- [46] W. Struyve, *Rep. Prog. Phys.* **73**, 106001 (2010).
- [47] B. A. Bassett, S. Tsujikawa, and D. Wands, *Rev. Mod. Phys.* **78**, 537 (2006).
- [48] J. H. Traschen and R. H. Brandenberger, *Phys. Rev. D* **42**, 2491 (1990).
- [49] R. Allahverdi, R. Brandenberger, F.-Y. Cyr-Racine, and A. Mazumdar, *Annu. Rev. Nucl. Part. Sci.* **60**, 27 (2010).
- [50] M. Endo, K. Hamaguchi, and F. Takahashi, *Phys. Rev. Lett.* **96**, 211301 (2006).
- [51] M. Kawasaki, F. Takahashi, and T. T. Yanagida, *Phys. Rev. D* **74**, 043519 (2006).
- [52] M. Endo, F. Takahashi, and T. T. Yanagida, *Phys. Rev. D* **76**, 083509 (2007).
- [53] F. Takahashi, *Phys. Lett. B* **660**, 100 (2008).
- [54] J. Ellis and K. A. Olive, in *Particle Dark Matter: Observations, Models and Searches*, edited by G. Bertone (Cambridge University Press, Cambridge, 2013).
- [55] L. Covi, *J. Phys. Conf. Ser.* **485**, 012002 (2014).
- [56] M. Fujii and T. Yanagida, *Phys. Lett. B* **549**, 273 (2002).
- [57] S. Nakamura and M. Yamaguchi, *Phys. Lett. B* **638**, 389 (2006).
- [58] S. Colin, [arXiv:1306.0967](https://arxiv.org/abs/1306.0967).
- [59] N. D. Birrell and P. C. W. Davies, *Quantum Fields in Curved Space* (Cambridge University Press, Cambridge, 1982).
- [60] L. Parker and D. Toms, *Quantum Field Theory in Curved Spacetime: Quantized Fields and Gravity* (Cambridge University Press, Cambridge, 2009).
- [61] C. Gerry and P. Knight, *Introductory Quantum Optics* (Cambridge University Press, Cambridge, 2004).
- [62] E. Jaynes and F. W. Cummings, *Proc. IEEE* **51**, 89 (1963).
- [63] L. I. Schiff, *Quantum Mechanics* (McGraw-Hill, New York, 1968).
- [64] G. Bertone, D. Hooper, and J. Silk, *Phys. Rep.* **405**, 279 (2005).
- [65] T. Bringmann, X. Huang, A. Ibarra, S. Vogl, and C. Weniger, *J. Cosmol. Astropart. Phys.* **07** (2012) 054.
- [66] C. Weniger, *J. Cosmol. Astropart. Phys.* **08** (2012) 007.
- [67] M. R. Buckley and D. Hooper, *Phys. Rev. D* **86**, 043524 (2012).
- [68] A. Ibarra, D. Tran, and C. Weniger, *Int. J. Mod. Phys. A* **28**, 1330040 (2013).
- [69] S. P. Liew, *Phys. Lett. B* **724**, 88 (2013).
- [70] A. Albert, G. A. Gómez-Vargas, M. Grefe, C. Muñoz, C. Weniger, E. D. Bloom, E. Charles, M. N. Mazziotta, and A. Morselli (Fermi-LAT Collaboration), *J. Cosmol. Astropart. Phys.* **10** (2014) 023.
- [71] F. Takayama and M. Yamaguchi, *Phys. Lett. B* **485**, 388 (2000).
- [72] M. Ackermann *et al.* (Fermi-LAT Collaboration), *Phys. Rev. D* **88**, 082002 (2013).
- [73] R. J. LeVeque, *Finite Volume Methods for Hyperbolic Problems* (Cambridge University Press, Cambridge, 2002).